CHARACTERIZING A NOVEL CONNECTION BETWEEN THE PLANT HORMONES CYTOKININ AND JASMONIC ACID IN CONTROL OF MAIZE LEAF GROWTH

A THESIS SUBMITTED TO THE GRADUATE DIVISION OF THE UNIVERSITY OF HAWAI'I AT MĀNOA IN PARTIAL FULFILLMENT OF THE REQUIREMENTS FOR THE DEGREE OF

MASTER OF SCIENCES

IN

TROPICAL PLANT AND SOIL SCIENCES

JULY 2018

By

Aimee Naomi Uyehara

Thesis Committee:

Dr. Michael G. Muszynski, Chairperson
Dr. Robert Paull
Dr. Miaoying Tian

Keywords: Maize, Jasmonic Acid, Cytokinin, *Hsf1,* Leaf Growth

ACKNOWLEDGMENTS

I would like to thank my advisor, Dr. Michael G. Muszynski for his mentorship, advice, and support in my academic pursuits. He has taught me much about the value of basic research (especially in genetics) and how to avoid “lugubrious ingeminations” with experimental design. Dr. Muszynski also puts the “fun” in functional genetics and I appreciate the time and effort invested into my project.

I am also grateful towards Dr. Angel Del Valle Echevarria for his mentorship and availability to answer my questions on top of all the other questions he receives. He guided the molecular genetics portion of my project and tirelessly walked us through new lab techniques. The *opr7, opr8* growth measurements were done in conjunction with Dr. Angel Del Valle Echevarria as well as much of the original manuscript editing. Thank you also to the Muszynski lab members for their help in collecting data and collaborators to the Muszynski lab for their patient advice over email.

Funding for this project was partially provided by the Syngenta Agricultural Scholarship.

Finally, I would like to thank my family and friends for their encouragement, and my husband, for listening to countless practice talks, bringing food for late lab nights, and bearing a greater proportion of household tasks during the thesis writing period.

The work presented here would not have been possible nor desirable without these people.

Aimee N. Uyehara

ABSTRACT

Plant growth is the accumulation of biomass over time and is due the combined effects of cell division and cell expansion. Understanding the molecular basis of plant growth in the context of the growth-defense tradeoff is important for agricultural sciences, and using a simple model to study growth enables this type of research. In *Zea mays L.* (maize), growth is spatially separated into three distinct growth zones making the maize leaf base a useful model for investigating growth on multiple scales. Mutants that affect maize leaf size are useful as an entry into the molecular networks guiding growth. The semi-dominant maize mutant, *Hairy Sheath Frayed (Hsf1)* is a CK hypersignaler with reduced leaf size, fewer dividing cells, and increased levels of the hormone jasmonic acid (JA) in the leaf growth zone. To determine if increased JA content in *Hsf1* contributes to its reduced leaf growth, the effects of JA on normal maize leaf growth were characterized. Our results showed that JA treatment dramatically reduced maize leaf size by reducing growth rate. Reduced JA content in the JA deficient *opr7, opr8* mutant led to increased leaf size mediated by an increased growth rate. Analysis of epidermal cell counts suggested that JA reduces cell proliferation rate, since cell size and density were not affected. Exogenous JA treatments of *Hsf1* indicated the mutant has a reduced response to JA. These data help explain the basis of growth reduction in *Hsf1* and set the foundation for further studies to uncover the players that mediate a novel interaction between CK and JA.

TABLE OF CONTENTS

LIST OF TABLES

LIST OF FIGURES

ABBREVIATIONS

CK	Cytokinin
Hsf1	*Hairy sheath frayed 1*
JA	Jasmonic Acid
LED	Leaf Elongation Duration
LER	Leaf Elongation Rate

INTRODUCTION

Plant Growth Regulators

Plant hormones are chemical cues that integrate external and internal signals that regulate growth, development, and physiology. These naturally occurring compounds function at low concentrations and are transported locally and systemically in the plant where they bind to their corresponding receptor to elicit a distinct biological response (Fré Bort, Kowalska, Hluska, Fré Bortová, & Galuszka, 2011). There are at least ten established plant hormones: abscisic acid (ABA), auxin (AUX), brassinosteroids (BR), cytokinin (CK), ethylene (ET), gibberellin (GA), jasmonate (JA), nitric oxide (NO), salicylic acid (SA), and strigolactones (SL) (Santner & Estelle, 2009). The relative abundance, conjugation, transport, perception, and catabolism of these hormones in model plant systems have been well described in different contexts (Santner & Estelle, 2009; Wang & Irving, 2011). Though specific hormones have been ascribed a predominant role in particular physiological and developmental processes, these processes cannot be achieved without the coordinated action of other hormones. The combinatorial interactions between hormone pathways, also called hormone crosstalk, enables a highly plastic biological response to a variety of inputs (Figure 1). Because plants are sessile organisms, it is particularly important they can balance growth demands with allocations to plant defense, such as those to pathogens and insect herbivores. Hormone crosstalk has been shown to play key roles in balancing resource investment between growth and defense to ensure plant survival.

The Growth-Defense Tradeoff

Plants need to balance the demands of growth and defense if they are to successfully reproduce. In the absence of pathogens, plant fitness, measured by plant biomass or number of seeds produced, has been shown to increase when defense pathways were silenced, and decrease when defense pathways were induced (Huot, Yao, Montgomery, & He, 2014). The exchange of growth for defense, or vice versa, has been coined the *growth-defense tradeoff*. This tradeoff proposes that, in a finite pool of resources the energy (i.e. sugars) invested in one process, such as growth, cannot be used in other

processes, such as defense, and vice versa, suggesting that investments into one will prevail at the expense of the other (Huot et al., 2014). The growth-defense tradeoff hypothesis was first suggested by Coley, Bryant and Chapin III in 1985 when they compared the success of plants in a range of environments and observed that slower growing plants succeeded in resource limited environments and experienced less herbivory than those in resource rich environments (Coley, Bryant, & Chapin III, 1985). Coley *et al.* (1985) speculated that the cost of regrowth in slow growing plants was higher than the cost of regrowth in faster growing plants, making it worthwhile for slow growing plants to synthesize more expensive anti-herbivory metabolites. They modeled plant growth rates as a measure of defense investment and hypothesized that an internal coordination of limited energy explained why slow growing plants had better anti-herbivore defense than fast growing plants (Coley et al., 1985).

Subsequent studies have traced the metabolic changes that occur upon pathogen infection or herbivory to show how limited resources are partitioned between growth and defense processes. The initiation of host resistance is accompanied by a reallocation of resources (e.g. transcriptional machinery, carbon in the form of sugars, and nitrogen) for incorporation into defense compounds and suppression of photosynthesis (Engelsdorf et al., 2013; Huot et al., 2014; Ullmann-Zeunert et al., 2013). If resources cannot be reallocated, such as in the *Arabidopsis* impaired starch metabolism mutants *phosphoglucomutase-1, pyrophosphorylase1-1,* and *starch excess1-1*, susceptibility to infection is increased (Engelsdorf et al., 2013).

From these experiments, the growth-defense tradeoff has been classically understood through a framework of a resource reallocation. However, recent studies indicate that the balance of growth and defense is established by preexisting hormone-regulated transcriptional networks (Campos et al., 2016; Huot et al., 2014). Thus, to understand plant growth and defense, understanding the underlying hormone networks is essential.

Plant hormones can be grouped by their associations with growth and defense processes. The main growth associated hormones are CK, AUX, BR, and GA. While many of these hormones have overlapping roles in plant growth and development, CK, AUX, BR, and GA are classically known for their roles cell proliferation, stem elongation, seed germination, and organ elongation, respectively (De Vleesschauwer, Xu, & Hofte, 2014). The main defense associated hormones are SA, JA, and ET (Huot et

al., 2014). SA regulates many plant immune responses, especially in regards to biotrophic pathogens while JA and ET often work in concert to antagonize SA signaling and induce wound responses (De Vleesschauwer et al., 2014; Huot et al., 2014). Growth hormones such as CK, AUX, and GA have been shown to crosstalk with various defense hormones to promote or suppress defense. For example, GA attenuates JA response through a 'relief of repression' model (Hou, Ding, & Yu, 2013). In the presence of JA, the JAZ proteins, repressors of JA response, are degraded, allowing JA transcription factors to bind and activate JA- responses. JAZ repressors are also bound by DELLA proteins, the repressors of GA signaling. The joint action of JA- mediated JAZ degradation and the competitive binding of JAZ by DELLAs facilitates the transcription of JA response genes. However, in the presence of GA, DELLA proteins are degraded and JAZ proteins become free to modulate JA response (Hou et al., 2013). Thus, defense responses mediated by JA are "fine-tuned" by GA, a classic growth regulating hormone.

Pathways for the Classical Hormone CK are Well Characterized

In the 1950s, Drs. Folke Skoog and Carlos Miller discovered cytokinin when they fortuitously isolated an active compound from autoclaved herring sperm that promoted cell proliferation in tobacco tissue culture (Amasino, 2005). Almost a decade later, the first naturally occurring cytokinin was discovered in maize (*Zea mays)* and named *zeatin* (Amasino, 2005). Cytokinins (CKs) are a highly diverse adenine-derived class of plant hormone that can be categorized into two classes based on the type of substitution at the N6 position (Figure 2A): (1) isoprenoid CKs carry an isoprene derived compound, while (2) aromatic CKs carry an aromatic side chain (Sakakibara, 2006). Different CKs have distinct biological functions dependent upon plant species, tissue type, and developmental stage (Sakakibara, 2006).

Biosynthesis, Conjugation and Catabolism

Isoprenoid CK biosynthesis is accomplished via two pathways: the methylerythritol phosphate (MEP) pathway located in the chloroplasts and the mevalonate (MVA) pathway located in the cytosol (Sakakibara et al., 2005). In the MEP pathway, ADENOSINE PHOSPHATE-ISOPENTENYL-TRANSFERASE (IPT) catalyzes the first step of CK biosynthesis by the N-prenylation (addition of a hydrophobic molecule) of an adenine precursor such as ADP or ATP to dimethylallyl diphosphate

(DMAPP) (Miyawaki et al., 2006; Naseem, Kaltdorf, & Dandekar, 2015; Sakakibara, 2006). The respective products, iP riboside 5' diphosphate (iPRDP) and iP riboside 5' triphosphate (iPRTP) are then hydroxylated by CYP735A into *trans*-zeatin nucleotides which are further processed in the CKs *trans*-zeatin, *cis*-zeatin, and dihydrozeatin (Sakakibara, 2006). N^6-(Δ^2-isopentenyl)adenine (iP) is also synthesized from iPRDP or iPRDP (Sakakibara, 2006). Once synthesized, bioactive CK nucleobases proceed to bind to a CK-receptor and activate downstream signaling. For maize, the CK receptor ZmHK1 is sensitive to both cZ and tZ, though cZs are the major type of CK in maize (Sakakibara, 2006).

Along this pathway are routes for inactivation and catabolism. CYTOKININ OXIDASE (CKX) catabolizes iP, tZ, and their nucleosides into adenine mainly in mature root and leaf tissue (Figure 2B) (Sakakibara, 2006). CKs can also be inactivated permanently through N-glycosylation and temporarily by O-glycosylation (Massonneau et al., 2004; Sakakibara, 2006). O-glycosylation generates a storage pool of CKs that are protected from CKX degradation by the sugar addition (Veach et al., 2003). In maize, *O*-glycosylation of cZ is mediated by the enzyme *cis*-ZEATIN *O*-GLUCOSYLTRANSFERASE (ZOG) encoded by the genes *cisZOG1* and *cisZOG2* (Martin, Mok, Habben, & Mok, 2001; Veach et al., 2003). Expression of *cisZOG1* and *cisZOG*2 is primarily in the roots (Figure 2B).

Transport

Local and systemic apoplastic transport of CKs enable plants to coordinate growth and developmental processes through the spatial and temporal separation of certain CKs from the site of their synthesis to the site of their perception (J. Kang, Lee, Sakakibara, & Martinoia, 2017). For example, tZ is more important for root meristem maintenance while iP must be translocated to the shoot to mediate vasculature development (Bishopp et al., 2011). Tissue and cell specific CK biosynthetic enzymes have been found to occur in both roots and shoots, and it is thought that CKs diffuse locally towards their target cells (Sakakibara, 2006). However, the presence of CKs in the xylem provides evidence for long-distance acropetal transport of tZs from the root to the shoot (Ko et al., 2014; Kudo, Kiba, & Sakakibara, 2010). Basipetal (shoot to root) transport of iP CKs is accomplished via the phloem as shown by the expression of CK responsive genes in the roots after CK treatment of plant shoots (Bishopp et al., 2011; Sakakibara, 2006). In the xylem, CKs are mostly transported in their nucleoside form and assisted by the

EQUILIBRATIVE NUCLEOSIDE TRANSPORTER (ENT) protein family, a protein that catalyzes selective transport of purines and nucleosides (Sakakibara, 2006).

Perception and Signaling

Perception and signaling of CK is mediated by a multi-step phosphorelay system that shares similar mechanisms to the prokaryotic two component signaling pathway (Ferreira & Kieber, 2005). For the multi-step phosphorelay of CK, a phosphoryl group is shuttled from histidine kinases (HKs) to histidine phosphotransfer proteins (HPs) in the cytoplasm which moves into the nucleus where the phosphoryl group is finally transferred to Response Regulator (RRs). Phosphorylation of Type-A and Type-B Response Regulators results in the suppression of CK signaling and transcription of CK response genes, respectively.

In plants, CK is perceived at the endoplasmic reticulum by a HK receptor, an intermembrane protein composed of three domains: a cytosolic binding domain, a histidine kinase domain, and a receiver domain (Figure 3A) (Lomin, Yonekura-Sakakibara, Romanov, & Sakakibara, 2011). Perception begins by CK binding to the CHASE (CYCLASES/HISTIDINE KINASE ASSOCIATED SENSORY EXTRACELLULAR) domain of the HK receptor, triggering autophosphorylation of the kinase domain. This begins the histidine to aspartate phosphorelay that results in the phosphorylation of a RR in the nucleus. *Arabidopsis* contains three CK receptors: *Arabidopsis* HISTIDINE KINASE2 (AHK2), AHK3, and AHK4 (Ferreira & Kieber, 2005). Maize also contains three CK receptors, listed here by respective homology to the aforementioned AHKs: ZmHK3a, ZmHK2, and ZmHK1 (Lomin et al., 2011). Similar to other plant HKs, ZmHK1 contains a CHASE domain between two hydrophobic membrane spanning domains, a histidine kinase domain, and a receiver domain, and transduction of the CK signal in maize follows the pathway conserved in all plants (Yonekura-Sakakibara, Kojima, Yamaya, & Sakakibara, 2004).

There are four classes of *Arabidopsis* response regulators (ARRs): type-A ARRs, type-B ARRs, type-C ARRs, and *Arabidopsis* pseudo-RRs. Type-A RRs encode a class of proteins that are some of the primary CK responsive genes (in the presence of CK, the transcription of these genes is activated immediately).The type-A RRs are negative regulators of CK signaling although how signaling is quenched is currently not known. (Ferreira & Kieber, 2005). Type-B RRs are the initial transcription factors that mediate early CK response but are only functional when phosphorylated (N. Y. Kang, Cho, & Kim, 2013;

Makino et al., 2000; To et al., 2007). Type-B RRs are nuclear-localized transcription factors whose transcriptional activation domain is suppressed by its receiver domain (Ferreira & Kieber, 2005). Transfer of the phosphoryl group from the HP to a type-B ARR relieves the repression, and allows type-B ARR mediated transcriptional activation of type-A ARRs and other CK responsive genes (Ferreira & Kieber, 2005). Importantly, a consensus DNA binding sequence of type-B RRs has been identified in the promoter region of many primary CK response genes (Ferreira & Kieber, 2005). This means that other genes which might be directly regulated by CK signaling, can be identified by the presence of the consensus type-B RR binding sequence in their promoters.

Biological Function: CKs are important regulators of growth and development

As mentioned before, CKs regulate a variety of plant growth and developmental processes such as shoot growth, apical dominance, and senescence. For this project, we focus on the growth function of CK in promoting cell division. In most cases, a reduction in CK signaling through loss-of-function mutants and transgenics, results in smaller plants. In *Nicotiana tabacum,* CK has been shown to be necessary for normal organ size by promoting cell division. In *Nicotiana tabacum* transgenic plants overexpressing the CK catabolic enzyme CKX (35S:CKX), CK levels were reduced, resulting in smaller plants with smaller leaves due to a reduced cell division rate and lower final cell count (Werner, Motyka, Strnad, & Schmülling, 2001). Interestingly, the final cell size of these transgenic plants was larger as compared to WT plants. These phenotypes suggest that a certain level of endogenous CK is necessary to promote a normal cell division rate and that the presence of CKs may contribute to determination of final cell size (Werner et al., 2001). Similar phenotypes are also observed when CK signaling was reduced/eliminated through the knockout of CK histidine kinase receptors via T-DNA insertion in *A. thaliana*. The triple loss-of-function *ahk2 ahk3 cre1* mutant exhibited an extreme miniaturization of the whole plant with smaller leaves that had fewer but larger epidermal cells (Riefler, Novak, Strnad, & Schmü Lling, 2006). However, the phenotypes of the triple mutant were accompanied by elevated levels of CK within the plant, suggesting that changes in CK signaling affect its homeostasis (Riefler et al., 2006).

Increased CK signaling results in larger plants in Arabidopsis

Constitutively active CK receptors in *A. thaliana* were discovered in the CK deficient *35S:CKX1* background in a suppressor screen of the CK deficiency phenotype (Schmülling et al., 2017). The gain-of-function *repressor of cytokinin deficiency2* (*rock2)* and *(rock3)* mutants exhibited larger leaves than wild types due to a 40-50% increase in leaf epidermal cell number, although cell size was slightly reduced (Schmülling et al., 2017). The authors concluded that the increase in plant size was due to a prolonged period of mitotic activity or a faster cell proliferation rate or both (Schmülling et al., 2017).

CK signaling in monocots

There are few CK biosynthetic and signaling mutants available in monocots. Previously, there was interest in the exogenous application of CK with the goal of improving crop yield. In rice, exogenous CK application has been shown to increase plant height and number of tillers (Zahir, Asghar, & Arshad, 2000). However, overexpression of the rice IPT gene, *OsIPT,* resulted in transgenic plants that did not grow over 1 cm tall and did not develop normal leaves. Instead, their leaf-like organs visually seemed to be composed mostly of sheath tissue (Sakamoto et al., 2006). These results suggest that an optimum concentration of CK is needed for normal plant growth and that too much CK results in stunted plants possibly following the bell shaped curve proposed for dicots by Ferreira & Kieber (2005). The *OsIPT* transgenic plants also reveal that CK plays a role in monocot leaf development.

Jasmonic Acid is a Key Hormone in Plant Defense

Jasmonic acid (JA) was first isolated from jasmine oil (*Jasminum grandiforum)* in 1962 by Demole, Lederer, and Mercier. Interested in this new fragrant compound, the perfume industry invested research into the volatile methyl ester of JA, methyl jasmonate (Creelman & Mullet, 1997). It was not until the1980s that interest in the role of JA as a plant growth regulator grew due to experiments showing growth reduction with exogenous application of JA (Ueda & Kato, 1982; Yamane, Sugawara, Suzuki, Shimamura, & Takahashi, 1980).

Biosynthesis, Conjugation and Catabolism

Jasmonic acid (JA) biosynthesis begins in the chloroplast with the release of chloroplast membrane phospholipids such as linolenic and alpha-linolenic acid by phospholipases (Lyons, Manners, & Kazan, 2013). Lipoxygenases catalyze the dioxygenation of the phospholipids forming the hydroperoxy octadecadienoic acids 13S-HPODE and 9S-HPODE which are then converted into 12-oxo phytodienoic acid (12-OPDA) via ALLENE OXIDE SYNTHASE (AOS) and ALLENE OXIDE CYCLASE (AOC) (Lyons *et al.* 2013). In the peroxisome, 12-OPDA is converted into (+)-7-iso-JA after reactions with 12-oxo-phytodienoic acid reductase (OPR) and three cycles of ß-oxidation (Lyons *et al.* 2013). From there, (+)-7-iso-JA is converted into various JA derivatives such as the bioactive form of JA: (3R,7S)-jasmonyl-L-isoleucine (JA-Ile) (Sheard et al., 2010; Y. Yan et al., 2012).

Transport

Upon wounding, many plants synthesize the JA precursors or JA-Ile, and can transport either JA-Ile or JA over both short and long distances (Tam Nguyen, Martinoia, & Farmer, 2017). A jasmonate transporter (JAT1), a member of the ABC transporter superfamily, has been discovered to export JA and JA-Ile across the plasma membrane and the nuclear envelope in *Arabidopsis* (Tam Nguyen et al., 2017).

Perception and Signaling

Perception of JA-Ile requires a co-receptor complex that includes the F-box protein CORONATINE INSENSITIVE 1 (COI1), the transcriptional repressor JASMONATE ZIM DOMAIN (JAZ), and inositol pentakisphosphate (Sheard et al., 2010). COI1 is part of the Skp1-Cul1-F-box protein

ubiquitin E3 ligase complex and contains the binding pocket for JA-Ile (Sheard et al., 2010). JA-Ile enters the COI1 binding pocket and the COI1-jasmonate complex then binds the JAZ1 degron (a short protein motif used by E3 ubiquitin ligases to target proteins for degradation) (Sheard et al., 2010). JAZ is then ubiquitinated and degraded by the 26S proteasome (Durand, Pauwels, & Goossens, 2016).

Under conditions where bioactive JA is absent, JAZ recruits other corepressors such as TOPLESS to repress MYC2, a basic helix-loop-helix transcription factor necessary for JA-mediated responses (Kazan & Manners 2013) (Figure 4).The presence of JA-Ile and the subsequent degradation of JAZ proteins by the SCF^{COI1}-JA-Ile-jasmonate ZIM-domain ternary protein complex releases MYC2, leading to downstream transcription and gene expression for plant defense and development processes (Hou et al., 2013; Y. Yan et al., 2012).

Biological Function: JA is necessary for defense responses to insect pests and pathogens

JA is synthesized in response to wounding by herbivorous pests or necrotrophic pathogens and is one mechanism in an array of common plant defense responses (Walling, 2000; Zhang & Turner, 2008). JA synthesis is used as a means of turning a localized signal into a systemic one (Huffaker et al., 2013). In *Arabidopsis*, repeated wounding induces the biosynthesis of JA, increasing endogenous JA levels, resulting in the upregulation of JA-responsive genes (Zhang & Turner 2008). Zhang and Turner (2008) showed that repeated wounding in *Arabidopsis* increased endogenous JA levels from 5 pmol/g to 391 pmol/g which resulted in a decrease in leaf area due to a reduction in mitotic index (Zhang & Turner 2008).

CK-JA Crosstalk, Cellular Locations and Interactions

A direct mechanism for JA-CK crosstalk has not been established and most of the literature describing any interaction comes from indirect evidence. One study implied a connection of CK signaling with increased defense against a necrotrophic pathogen by showing that type-B ARRs interact directly with SA response genes (Choi et al., 2010). A review by Muhammad Naseem (2015) connected elevated CK levels with increased resistance to necrotrophic pathogens in tobacco, *Arabidopsis*, and tomato

(Naseem et al., 2015). While not describing CK-JA crosstalk directly, these studies suggest a role for CK in modulating plant defense.

A study in maize also indirectly points to possible CK-JA crosstalk. Over expression of zeatin *O*-glucosyltransferase (*ZOG1*) in transgenic *Ubi:ZOG1* maize lines resulted in elevated levels of *O*-glucosylzeatin and a subsequent increase in CK biosynthesis in the leaves (but not necessarily an increase in CK activity) (Rodo et al., 2008). *O*-glucosylzeatin is a CK derivative formed through the addition of a sugar on the *O* of the side chain. The addition of the sugar moiety to zeatin inactivates the CK until hydrolyzed by ß-glucosidase and protects it from degradation by CK oxidases and dehydrogenases (Rodo et al., 2008). Homozygous transformants overexpressing *ZOG1* showed CK deficiency phenotypes as well as a feminized tassel (Rodo et al., 2008). While it is difficult to determine if the tasselseed formation is due to less or more active CK, the researchers also reported tasselseed formation in a transgenic overexpressing CKX (Rodo et al., 2008). These results are interesting because tasselseed is a distinctive phenotype of JA deficiency in maize and the presence of this phenotype in transgenic lines overexpressing CK catabolic enzymes indicates a role of CK in feminizing tassels, potentially through the JA pathway.

A Brief Comparison of CK and JA Signaling in Monocots and Dicots

Monocots diverged from the dicot lineage about 140-150 million years ago in the late Jurassic or early Cretaceous period (Chaw, Chang, Chen, & Li, 2004). However, key components of both the CK and JA biosynthesis and signaling pathways have been preserved in both monocots and dicots (Frebort, Kowalska, Hluska, Frebortova, & Galuszka, 2011; Han, 2016). The influence of CK and JA on plant growth can be seen early in the evolutionary history of plants before the monocot-dicot divergence. The first CKs in simple plants were the products of decomposed tRNA molecules (Fré Bort et al., 2011). To increase the pools of available CK, CK biosynthesis genes evolved in flowering plants possibly as a way to overcome the limitations of tRNA decomposition (Frebort et al., 2011). Thus, complete CK biosynthesis pathways are conserved in flowering plants while CK signaling pathways are conserved from early basal land plants (Fré Bort et al., 2011). JA was also present early in the evolution of plants, but the pieces

necessary for JA signaling were not present until land plants diverged from the charophytes (Han, 2016). Therefore, land plants but not algae contain the key components of JA biosynthesis and signaling (Han, 2016).

Due to the availability of mutants, much of the research identifying components of the CK and JA pathways has been done in the model eudicot *Arabidopsis*. The mutants in *Arabidopsis* used to define the CK biosynthesis and signaling pathways include *ipt1/3/5/7*, *ahk4/cre1/wol1*, *ahp1/2/3/4/5/6*, and *arr1/2/10/11/12* (Ferreira & Kieber, 2005). The core biosynthesis and signaling components are conserved in all flowering plants, although the number of paralogs varies by species (Fré Bort et al., 2011). Few CK mutants have been isolated in maize so far with only the recessive type-A RR mutant *aberrant phyllotaxy1* (*abph1*) and the semi-dominant, gain-of-function ZmHK1 mutant *Hsf1* described. The identification of JA mutants in *Arabidopsis* was also critical to the definition of the JA biosynthesis and signaling pathways (Han, 2016; Xie, Feys, James, Nieto-Rostro, & Turner, 1998). The JA biosynthesis pathway was defined by *fad3/7/8, opr3/dde1, aos/dde2* mutants and the signaling pathways by the *coi1, jin4/jar1,* and *jin1/myc2* mutants (Yuanxin Yan, Huang, Borrego, & Kolomiets, 2014). Where examined, the core JA biosynthesis and signaling pathways are also conserved in flowering plants (Han, 2016). Only a few JA mutants in monocots exist and in maize these include the *opr7, opr8* double mutant and the *tasselseed1* (*ts1*) mutant. Along with decreased defense responses, these mutants also display changes in development, like a feminized tassel, along with other growth defects.

Maize Leaf Growth

The Maize Leaf is a Simple Model for Studying Growth

There are three identifying stages in maize leaf development: 1) organogenesis, 2) primary morphogenesis, and 3) leaf differentiation (Sylvester, Smith, & Freeling, 1996). Organogenesis occurs at the shoot apical meristem (SAM), with the formation of founder cells, a group of progenitor cells that have “limited cell fates”, on the flanks of the SAM (Poethig, 1984). Organogenesis gives rise to the emerging leaf primordia. Primary morphogenesis describes the stage where the founder cells divide to form leaf primordia proper. During this stage, the three main growth axes are established: proximal-distal, medial-

lateral, and abaxial-adaxial (Du, Guan, & Jiao, 2018). Primary morphogenesis results in the primordia taking on the basic shape of the leaf. Leaf differentiation defines the stage where the majority of growth and differentiation occurs. In maize, like all grasses, cell division, elongation and differentiation are spatially separated along the proximal-distal growth axis. All the biomass producing cell divisions occur at the base of the leaf. Distal to this region is an area of cell elongation, and distal to the elongation region is where cells differentiate and take on their final fates. On the epidermal surface, this gradient of cell types can be seen as proliferative cell divisions at the base that transition into formative cell divisions before cells become fully differentiated (Sylvester et al., 1996)

The first leaves initiated on the maize shoot form during embryogenesis (Kiesselbach, 1999; Vernoud, Hajduch, Khaled, Depège, & Rogowsky, 2005). Upon maturation, the maize embryo contains two specialized “leaves” and four to five leaf primordia surrounding the shoot apical meristem (SAM). The scutellum is the outermost modified leaf that functions to assist with the digestion of the endosperm during germination. Surrounding the embryonic shoot axis is the second specialized leaf, the coleoptile, which is modified to protect the inner well-organized whorl of four to five foliage leaf primordia (Kiesselbach, 1999).

Upon germination, the growth and development of the pre-formed leaves in the embryo continues. At stage three in development, the maize leaf can be partitioned into distinct and spatially divided growth zones: a division zone, expansion zone, and a maturation zone (Nelissen et al., 2013; Sylvester et al., 1996). This is useful because growth is a function of cell division and cell expansion and these aspects of growth can be visualized in a spatial continuum by using the maize leaf (Figure 5).

In maize, the growth of the leaf begins basally at the point at which the leaf inserts into the node. As the cells near the base are displaced distally by the basal cell divisions of the intercalary meristem, epidermal cell morphology changes from the small rectangular block shape characteristic of dividing cells to the elongated, crenulated (irregularly wavy) mature cells. Leaves can be sampled, fixed, stained, and visualized throughout growth to take growth zone measurements. Using these unique morphological characteristics of the leaf epidermal cells, the growth zones can be identified and measured for kinematic analysis (Nelissen et al., 2013).

The *Hairy Sheath Frayed1* Mutant Affects Leaf Growth

The *Hairy sheath frayed1 (Hsf1)* mutation was first identified in 1985 in the collection of Dr. M.G. Neuffer's ethyl methanesulfonate (EMS) mutants as a very hairy plant that formed ectopic sheath tissue along the leaf blade margin (Bertrand-Garcia & Freeling, 1991). Characterization of the semi-dominant *Hsf1* mutant resulted in the identification of three key leaf phenotypes (Figure 6): (1) shorter and narrower leaf blades, (2) excessive presence of macrohairs, especially on the abaxial sheath and blade margins, and (3) the presence of ectopic outgrowths along the blade margin consisting of proximal sheath tissue (called "prongs") (Bertrand-Garcia & Freeling, 1991; Cahill, 2015).

Hairy Sheath Frayed1 is a Cytokinin Hypersignaling Mutant with Reduced Growth

The initial phenotypic characterization of *Hsf1* showed changes to leaf growth, cell fate, and organ formation (Bertrand-Garcia & Freeling, 1991). Later, the gene underlying *Hsf1* was shown to be one of the maize CK receptor genes *Zea mays Histidine Kinase 1* (*ZmHK1)* (Muszynski et al., unpublished). Characterization of three *Hsf1* mutant alleles indicated that the mutant phenotype was due to specific missense mutations in the CK receptor that caused CK hypersignaling which was validated by yeast two hybrid analysis (Muszynski, unpublished).

Consistent with this hypothesis, germinating seed CK treaments in maize phenocopies the *Hsf1* mutant (Figure 7). Plants show stunted growth, smaller leaves, macrohairs on the abaxial side of the blade, and prong outgrowths from the blade margins (Cahill, 2015).

CK is known to promote cell proliferation in shoot tissue (Eric Schaller, Street, Kieber, & Eric, 2014). Previous experiments have shown that smaller plants were the result of reduced endogenous CK (Werner et al., 2001) and gain-of-function mutations in the *Arabidopsis* HKs result in bigger plants (Schmülling et al., 2017). However, the growth phenotypes observed in *Hsf1* were surprising and we hypothesized that the mutation in *ZmHK1* may have revealed a novel crosstalk between CK and another hormone.

Hormone Profiling and Kinematic Analysis of *Hsf1* Suggests a Role of JA in Reducing Growth

Arabidopsis plants have been shown to make smaller leaves upon induction of JA biosynthesis by reducing the leaf mitotic index (the ratio of mitotic cells out of all cells) (Zhang & Turner, 2008). Two-week old whole-seedling hormone profiles indicated that JA levels in *Hsf1/+* were elevated as compared to the WT-sibling while other hormones showed no significant difference (Figure 8A) (Jander *et al.,* unpublished data). To understand the spatial scale of JA accumulation across the leaf, leaf six was divided into three sections (base, middle, and tip) to measure JA levels at steady state growth. JA levels were higher in the *Hsf1/+* mutant across the whole leaf, including the growth zone contained in the leaf base as compared to WT siblings (Figure 8B) (Hunter *et al.,* unpublished data). In addition, *Hsf1/+* also showed increased resistance to caterpillar and insect feeding (Figure 9) (Jander *et al.*, unpublished data).

Growth is a function of cell division and expansion, and in the maize leaf, cell division and cell expansion can be separated into distinct and spatially separated growth zones (Nelissen et al., 2013). Kinematic analysis is a useful means for measuring the individual roles of division and expansion. Growth zone size, the number of cells within each zone, and the rates of division or expansion can all be determined by kinematic analysis to understand leaf growth at the cellular level (Nelissen et al., 2013). Knowing that JA reduces the number of dividing cells in *Arabidopsis*, a closer examination of the *Hsf1/+* growth zones was needed. Kinematic analysis of *Hsf1/+* leaf #4 indicated that *Hsf1*/+ leaves were smaller than WT sibs due to a reduction in the size of their division zone because they contained less dividing cells (Table 1) (Nelissen *et al.,* unpublished data).

Leaf elongation rates (LERs) of leaf #4 were also taken (Figure 10). LERs are the changes in leaf growth over time taken from when leaf #4 emerges from the whorl until growth is complete. Leaf elongation duration (LED) is a measure of time defined from when the leaf is 10 cm until it has completed growth (Sun et al., 2017). LERs provide information on the underlying cellular components of growth. For example, differences in LER are usually due to a difference in division zone size while differences in leaf elongation duration (LED), are due to the extended presence of a division zone (Sun et al., 2017). Leaf #4 growth rates showed that *Hsf1*/+ has smaller LER and a longer LED compared to WT (Figure 10). Altogether, these results implicate a JA-mediated mechanism for smaller leaves downstream of CK signaling.

The higher concentrations of JA in the *Hsf1/+* growth zone in combination with its smaller division zone implicate a JA-mediated mechanism for smaller leaves downstream of CK signaling. However, the effects of exogenous JA application in maize has not been performed and therefore a characterization of JA application on maize must be established for further dissection of the CK-JA crosstalk and how it relates to growth.

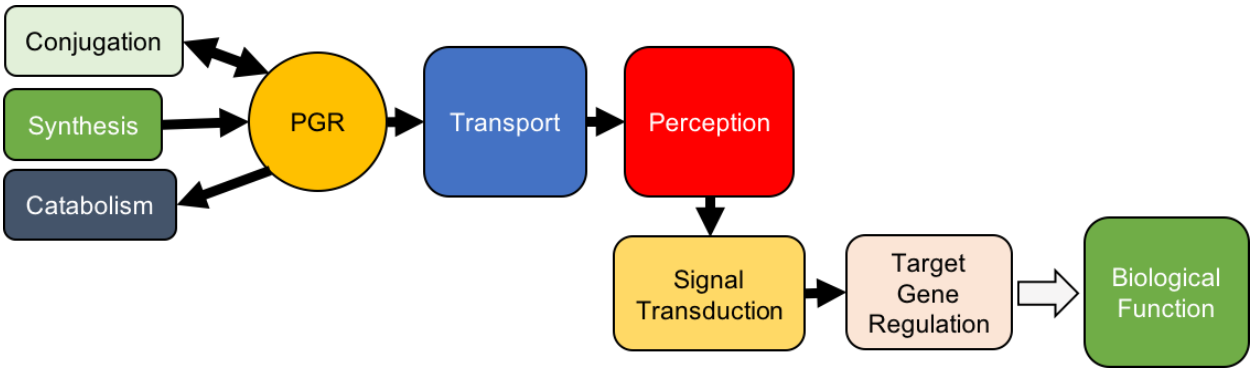

Figure 1. General plant growth regulatory pathways from synthesis to biological function. PGR, Plant growth regulator; TF, transcription factor. Figure modified courtesy of Dr. Robert Paull (University of Hawai'i at Mānoa).

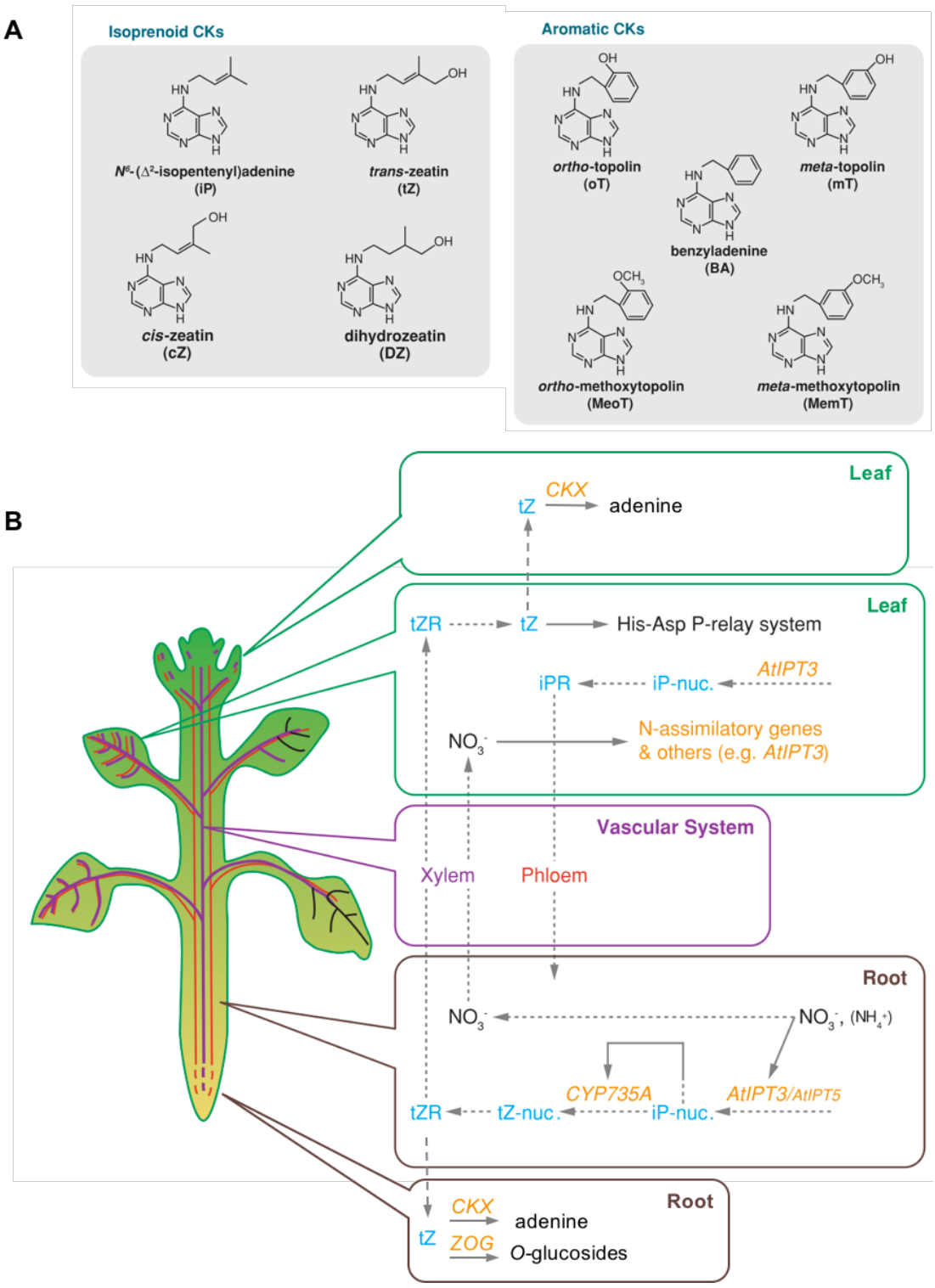

Figure 2. CK structure and location modified from Sakakibara, 2006. (A) CKs are grouped into isoprenoid and aromatic CKs. (B) Locations biosynthesis, transport, and catabolism of tZ. Figure modified from Sakakibara, H. (2006). Cytokinins: Activity, Biosynthesis, and Translocation. Annu. Rev. Plant Biol, 57, 431–49. http://doi.org/10.1146/. Panel B has been modified to include CKX and ZOG.

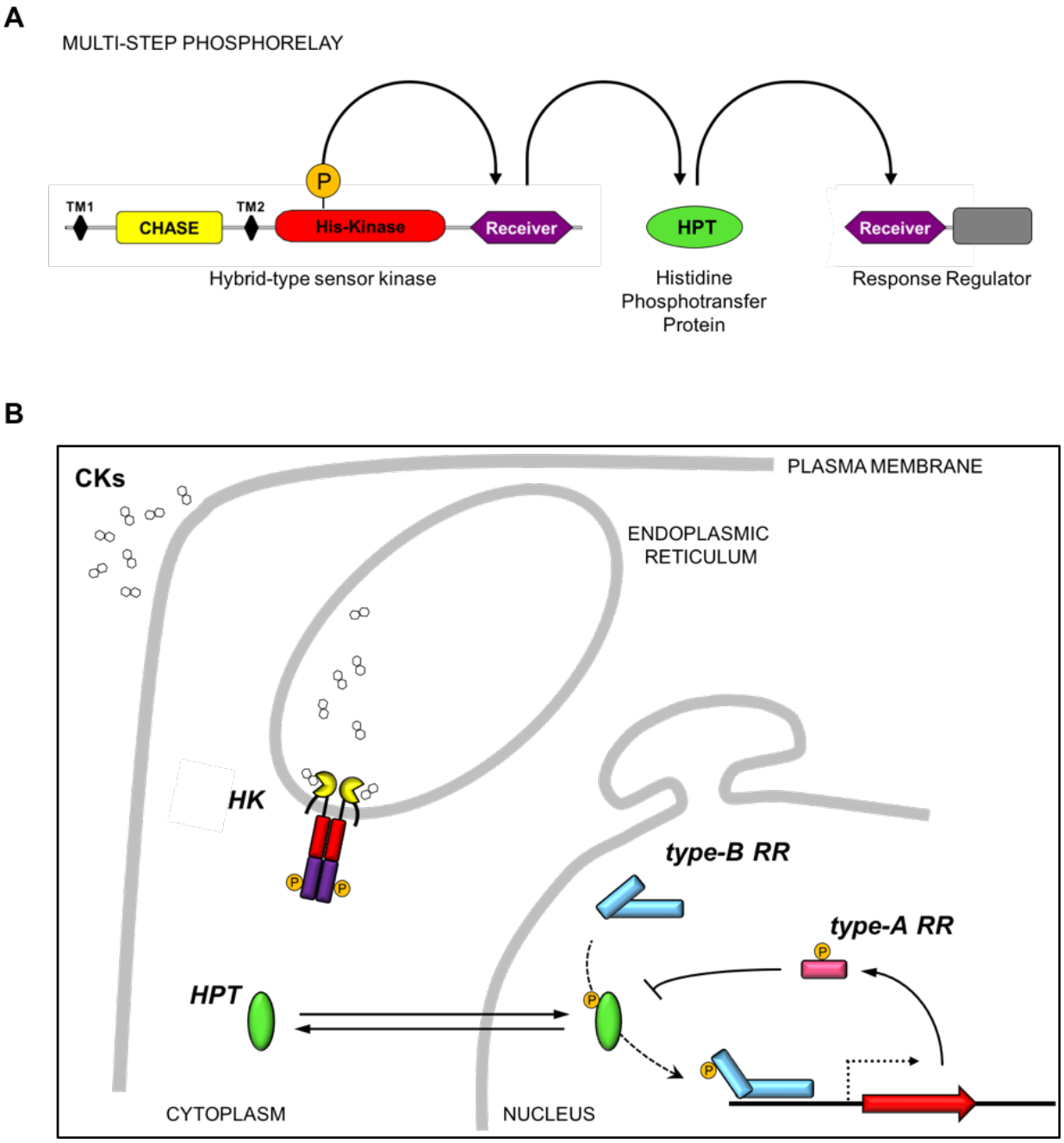

Figure 3. Perception and signaling of CK in *Arabidopsis*. (A) The CK multi-step phosphorelay contains three parts: a hybrid-type sensor kinase, a histidine phosphotransfer protein, and a response regulator. Modified from Ferreira, F. J., & Kieber, J. J. (2005). Cytokinin signaling. Current Opinion in Plant Biology, 8(5), 518–525. http://doi.org/10.1016/J.PBI.2005.07.013. (B) CK perception at the histidine kinase CHASE domain results in the autophosphorylation at the kinase domain. This begins the histidine to aspartate phosphorelay that results in the phosphorylation of a response regulator. Figure modified courtesy of Dr. Michael Muszynski (University of Hawai'i at Mānoa).

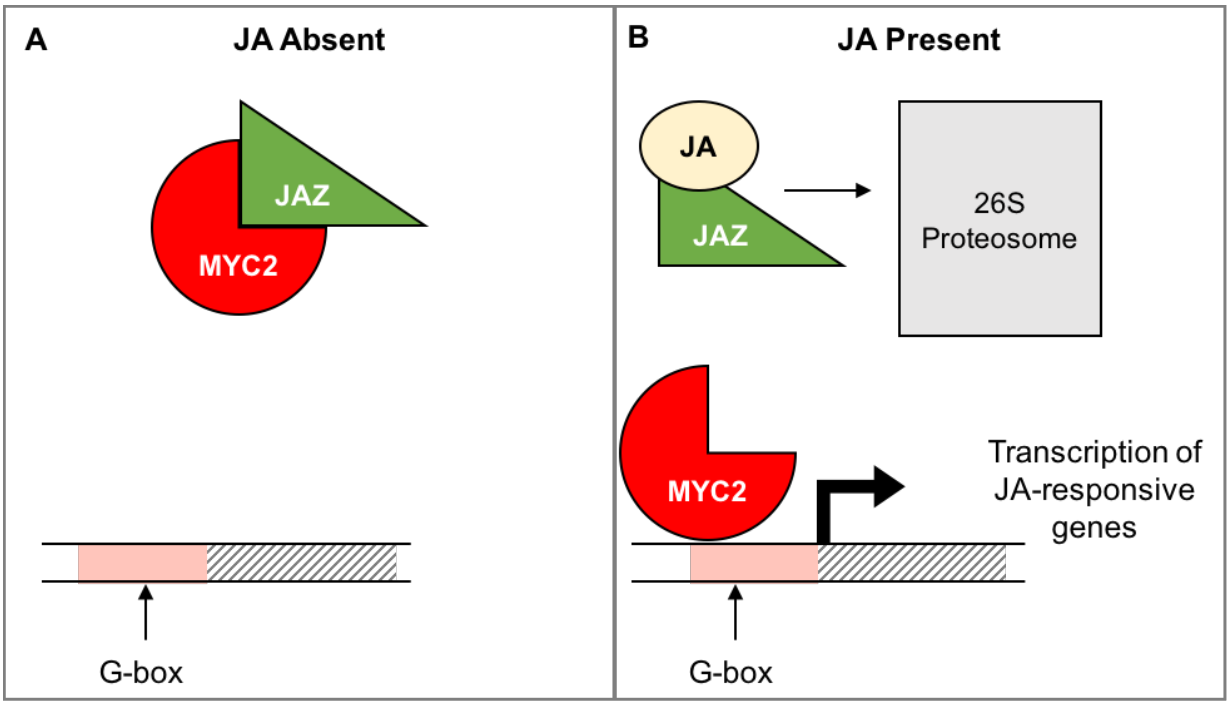

Figure 4. Transcriptional activation of JA-responsive genes modified from Figure 1 in Hou, Ding, Yu, 2013. In the absence of JA (A), JAZ binds to MYC2, preventing MYC2 from binding to the G-box and activating JA signaling. (B) JAZ is destabilized in the presence of JA and degraded in the 26S proteosome. Degradation of JAZ allows MYC2 binding of the G-box and activation of JA responsive genes.

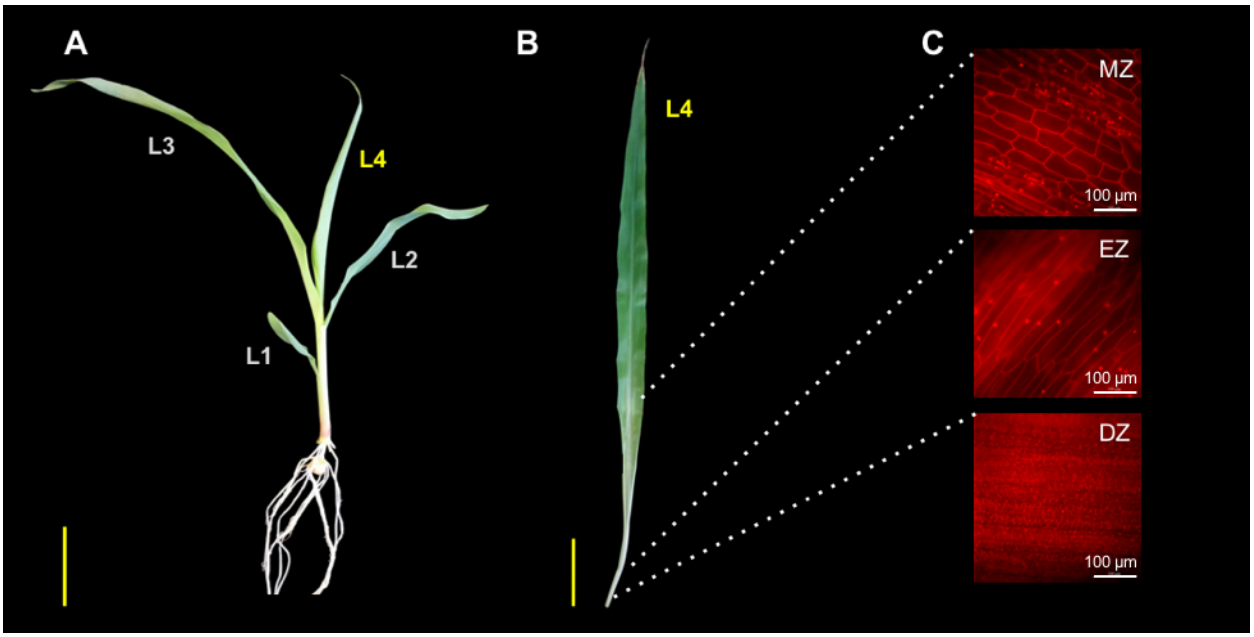

Figure 5. Growth in maize leaves is restricted to the leaf base. (A) 13-day old B73 seedling with 4 visible leaves (L1 – L4). (B) Leaf #4 (L4), dissected from the B73 seedling in (A), is at steady-state growth. Yellow scale bars are 5 cm. (C) Propidium iodide stained sections from the division (DZ), elongation (EZ) and maturation (MZ) zones from L4. Scale bars are 100 µm for each zone.

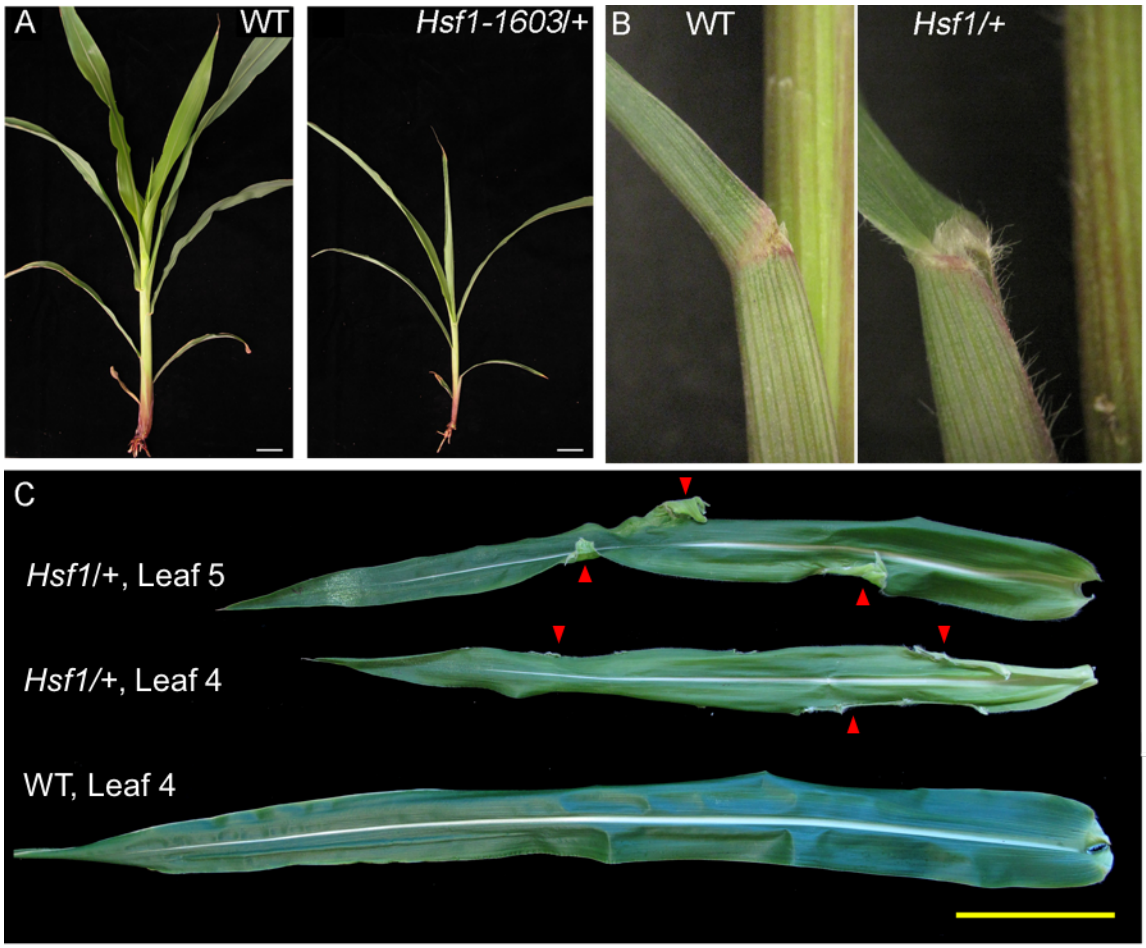

Figure 6. *Hsf1-1603/+* has three distinctive characteristics. (A) *Hsf1/+* is stunted in size compared to its WT sibling. Scale bar is 5 cm. Picture courtesy of James Cahill. (B) Abaxial macrohairs give *Hsf1/+* its name and fuzzy texture compared to WT. Picture in A and B are courtesy of James Cahill. (Iowa State University) (C) The 4th and 5th leaves from a mature *Hsf1-1603/+* plant compared to WT show prong formation along the leaf margin (red arrows). Scale bar is 10 cm. Picture courtesy of Dr. Angel Del Valle Echevarria (University of Hawai'i at Mānoa).

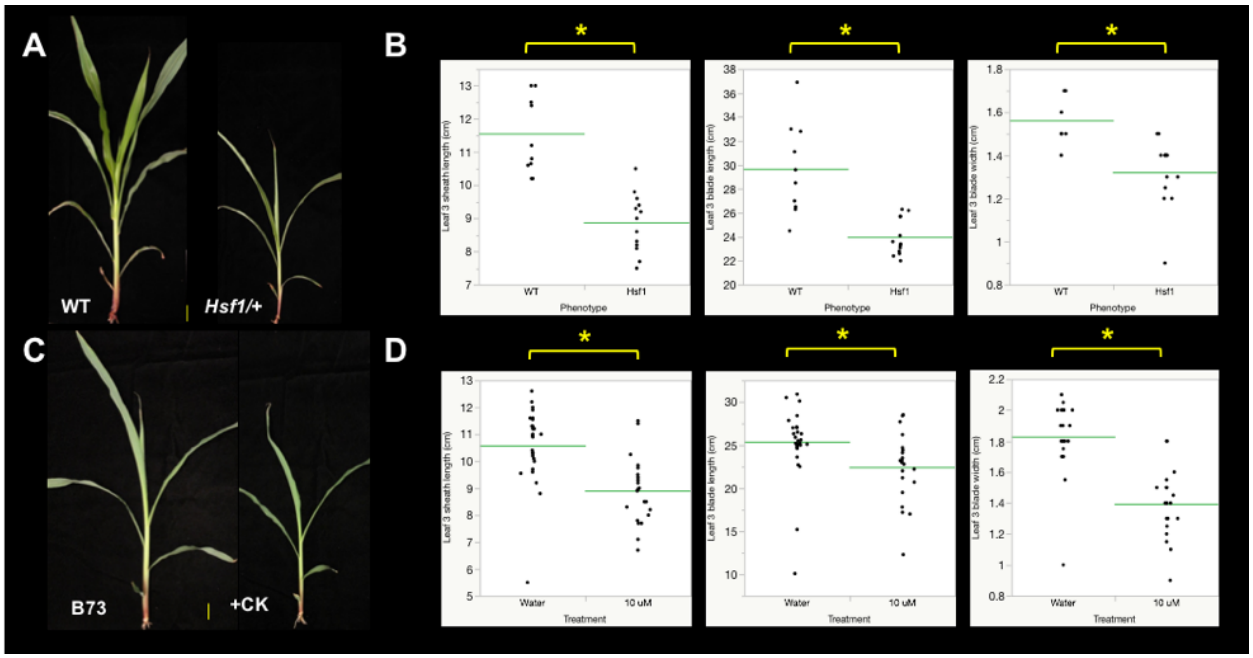

Figure 7. Growth is reduced in *Hsf1* and by CK treatment. (A) 3-week old *Hsf1/+* and wild type (WT) sib seedlings. (B) *Hsf1/+* sheath and blade length, and blade width are significantly reduced compared to WT siblings. (C) 3-week old B73 seedlings following a six-day germinating seed reatment with CK (10 μM 6-benzylaminopurine, 6-BAP). (D) 6-BAP treatment mimics the inhibited leaf growth of the *Hsf1/+* mutant. The yellow scale bar is 3 cm. A dot represents one leaf, the green bar is the mean, and the asterisk indicates a p-value ≤ 0.05 calculated from a two-tailed Student's t-test.

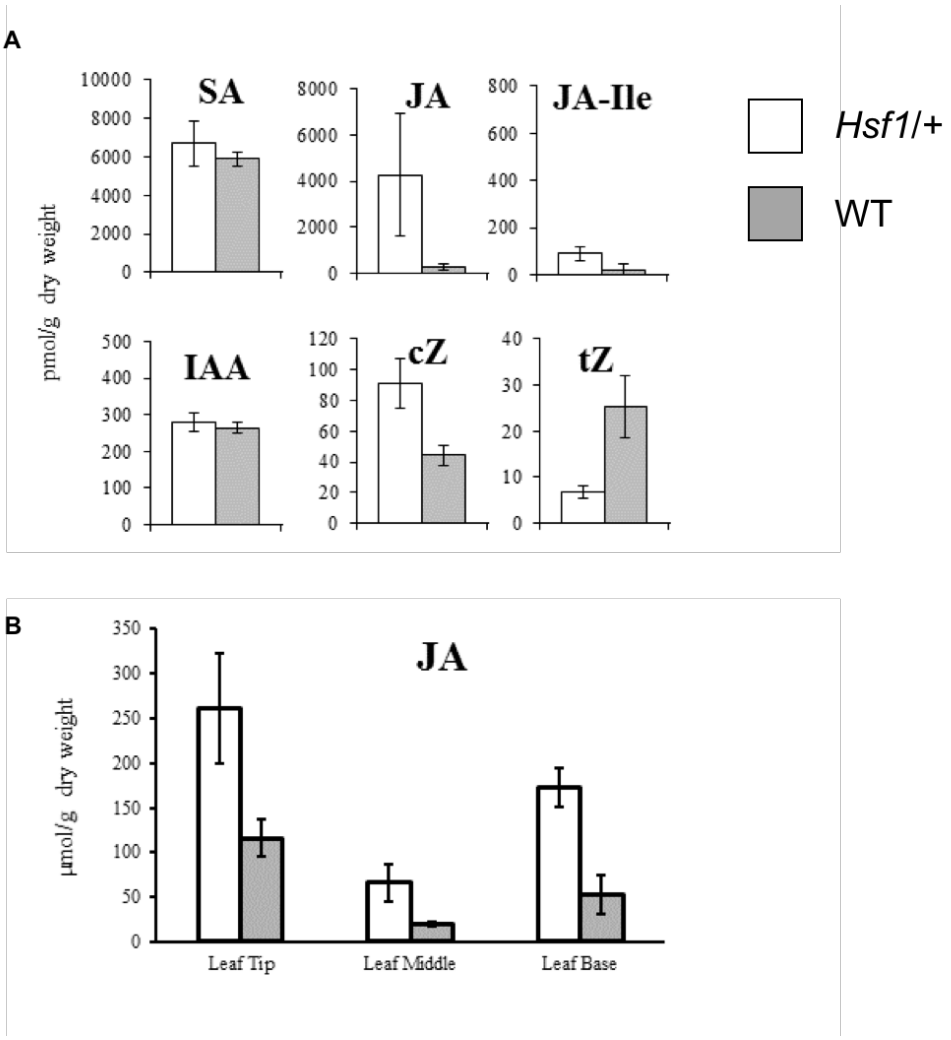

Figure 8. Hormone profile of *Hsf1/+* and WT-siblings. (A) Whole-seedling hormone profile. SA, Salicylic Acid; JA, Jasmonic Acid; JA-Ile, Jasmonic Acid Isoleucine; IAA, Indole-3-Acetic Acid; cZ, *cis*-Zeatin; tZ, *trans*-Zeatin. (B) Jasmonic Acid (JA) profile across leaf six. Leaf at steady state growth was divided into three sections (leaf base, leaf middle, leaf tip). Leaf base includes the division zone, elongation zone, and part of the maturation zone. White columns are *Hsf1/+* and gray columns are WT-sibling. Data in A is courtesy of Dr. Georg Janders (Boyce Thompson Institute) and in B courtesy of Dr. Charles Hunter (USDA Center for Medical, Agricultural and Veterinary Entomology).

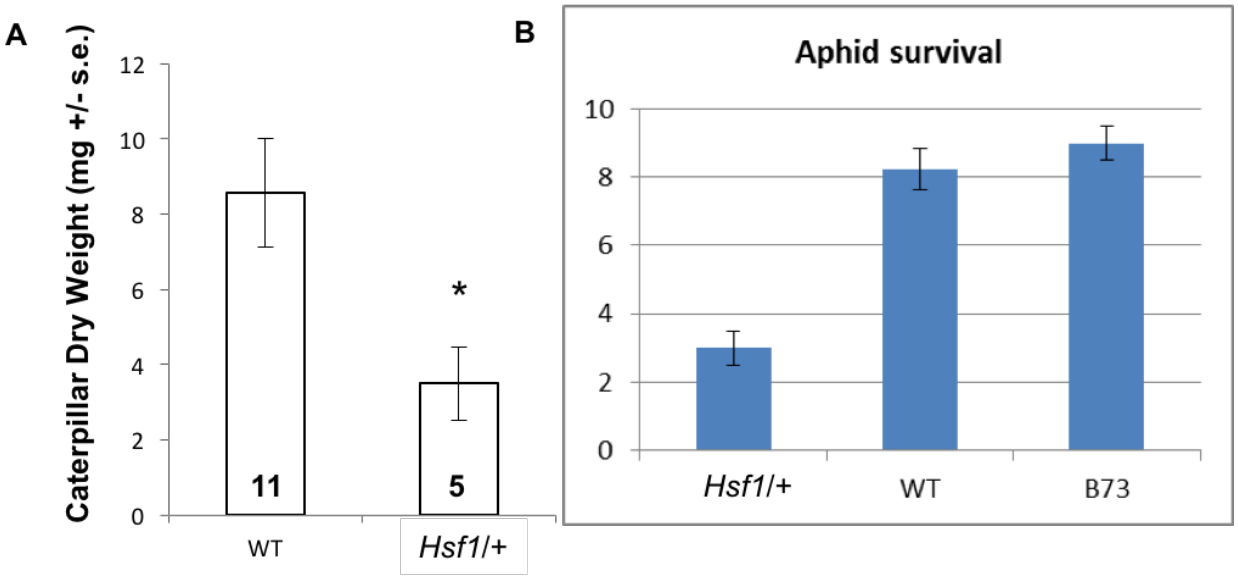

Figure 9. Hsf1/+ shows resistance to caterpillar and aphid feeding. (A) Caterpillar dry weight after feeding on two-week old *Hsf1/+* and WT-sib seedlings. (B) Aphid survival after feeding on two-week old *Hsf1/+*, WT sibs, and B73 inbred seedlings. Data courtesy of Dr. Georg Janders (Boyce Thompson Institute).

Table 1. Growth zone sizes and cell counts for *Hsf1/+* and WT-siblings. The division zone is significantly reduced in *Hsf1/+* compared to WT due to a significant reduction in the number of dividing cells in seedling leaf #4 at steady state growth. Data courtesy of Dr. Hilde Nelissen (VIB).

	Wild Type	Hsf1/+	P-value
Length Division Zone (cm)	1.044 ± 0.04	0.84 ± 0.48	0.003
Dividing Cell Size (µm)	16.52 ± 7.42	16.93 ± 1.06	0.819
Number of Dividing Cells	646.28 ± 56.57	511.56 ± 47.11	0.049
Length Elongation Zone (cm)	5.969 ± 0.47	4.21 ± 0.13	0.089
Elongating Cell Size (µm)	91.235± 2.00	86.90± 4.22	0.329
Number of Elongating Cells	702.80± 77.22	645.11± 27.34	0.333
Mature Cell Size (µm)	150.46 ± 10.39	138.73 ± 4.62	0.185

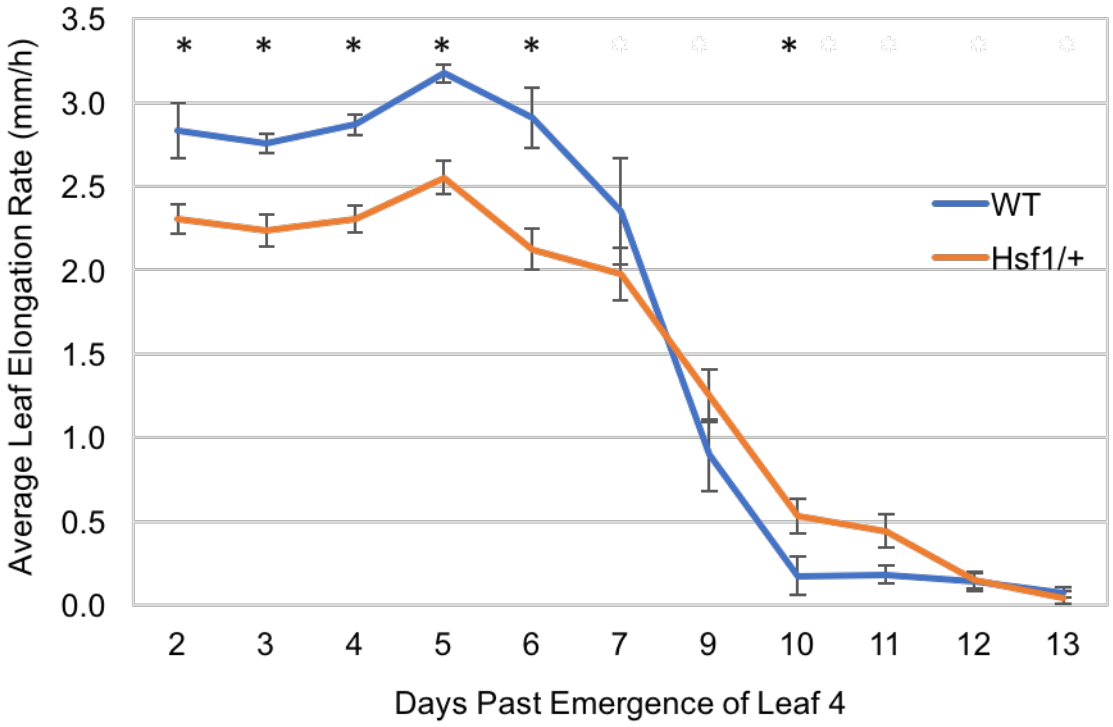

Figure 10. LER of leaf #4 from *Hsf1/+* and WT-sib seedlings. Asterisks mark significant difference p ≤ 0.05. Error bars are standard error.

HYPOTHESIS AND OBJECTIVES

Based on results from previous studies and our own unpublished results, we hypothesize that CK promotes JA accumulation to modulate cellular processes to control growth. We propose that increased CK signaling, either by exogenous CK treatment or in the *Hsf1* mutant, leads to increased JA levels which suppress cell divisions resulting in reduced leaf growth. To test these ideas, the effects of JA on growth in normal maize and the *Hsf1* mutant needed to be characterized. Thus, the following three objectives were designed.

1. Determine the effects of JA application on normal maize leaf growth.
2. Determine the cellular changes in the maize leaf growth zone due to exogenous JA treatment.
3. Determine the effects of exogenous JA application on maize leaf growth in the *Hsf1* mutant.

RESULTS

Objective 1: Determine the effects of JA application on normal maize leaf growth.

JA Treatment Reduces Leaf Size

JA has been studied predominantly in plant defense, but few studies have focused on its role in plant growth (Zhang & Turner, 2008). JA related compounds have been shown to inhibit rice seedling growth (Yamane et al., 1980). However, the effects of exogenous JA application on maize growth have not been examined previously. To determine if JA treatment reduced leaf growth, maize seeds were germinated in a 1 mM JA solution using a modified germinating seed hormone treatment from J.C. Cahill (2015, see Materials & Methods). Briefly, imbibed inbred seed was incubated with the JA treatment solution, in the dark, for 6 days. After that time, the emerging seedlings were rinsed, planted in pots in the greenhouse and left to grow until the four basal seedling leaves were fully mature (ca. 2-3 weeks). Three parts of the maize leaf were measured: sheath length (distance from the leaf insertion point to the ligule), blade length (distance from the ligule to the blade tip along the midrib), and blade width (width of the blade at half the blade length) (see Materials & Methods). The total leaf length is the sum of the sheath and blade lengths. These measures were used as an estimate of leaf size.

After the transient 1 mM JA treatment, B73 seedling leaves one through four (#1 - #4) were significantly reduced in size, including sheath length, blade length, and blade width (Figure 11). Leaf #1 was reduced the most in size (20-30%) compared to leaves #2 - #4 (Table 2) and was obviously visually smaller when compared to control plants (Figure 12). Leaf blade and sheath length were reduced 26-30% while blade widths were reduced 9-20% (Table 2). As leaf number increased, the growth-inhibiting effect of JA declined (Figure 11). These results show that an exogenous 6 day 1 mM JA treatment reduced final leaf size in B73 seedlings.

Perception of JA Treatment is Time and Leaf Number Dependent

Final growth effects of the previous 1 mM JA treatments were observed after 6 days of treatment. To find the minimum length of JA treatment time needed to affect leaf growth, a JA time course was done on B73 seed. Following the standard germinating seed hormone treatment (See Methods), B73 seeds were treated with 1 mM JA for 1, 6, 12, 24, and 48 hours (Figure 13). All final leaf size measurements were taken after leaf #4 had completed growth, 2-3 weeks later following hormone treatment. The effect of JA was dependent upon the leaf measured and the length of treatment. A 24-hour treatment time was sufficient to cause a decrease in final leaf blade length in leaf #1 (Figure 13A, Blade Length), whereas a 48-hour treatment time was needed to reduce sheath length and blade width in leaf #1 (Figure 13A). Leaf #2 blade length and width were reduced after 48 hours of JA treatment (Figure 13B). But leaf #2 sheath length was not affected by any of the treatment times. For leaf #3, blade length and blade width were reduced after 48 hours of JA treatment (Figure 13C). Leaf #4 did not show any significant effect of JA treatment up throughout the time points tested (Figure 13D).

After 48 hours of JA treatment, the percent reduction in leaf #1 blade length neared 30% (Table 3) which is the percent reduction observed after 6 days of 1 mM JA treatment (Table 2). Thus, for leaf #1 blade length, a 48-hour JA treatment was sufficient to cause an equivalent degree of growth reduction as the 6-day treatment. The growth reducing effect of JA treatment declined as leaf number increased. Forty-eight hours of 1 mM JA treatment reduced growth in leaves #1 to #3, but was not long enough to affect leaf #4. The minimum length of time needed to reduce growth in leaves #1 to #4 would fall between 48 hours of treatment and 6 days of treatment. Therefore, a treatment length of 6 days was used for our other studies.

JA response is Dose Dependent

Previous experiments with other plant species used exogenous JA at concentrations of 10 μM to 1 mM (Creelman & Mullet, 1997; Yamane et al., 1980; Y. Yan et al., 2012). To test if leaf growth reduction was JA-dose dependent, B73 maize seeds were treated with 10 μM, 100 μM, and 1 mM JA, and their respective controls, using the standard 6-day seed treatment assay (Figure 14). The 10 μM and 100 μM treatment had no significant effect on final leaf size in leaves #1 to #4. However, as the concentration of JA increased, a reduction in size, albeit insignificant, was observed for all concentrations in blade length measurements. Only the 1 mM JA treatment showed significant changes in leaf size compared to the control across all four leaves, consistent with studies published for other plant species and our previous experiment (Figure 11).

Leaf Elongation Rate is Reduced by JA Treatment

To identify the process(es) underlying JA-mediated reduced leaf size, the effects of JA treatment on leaf elongation rate (LER) and leaf elongation duration (LED) were determined. To do this, B73 seeds were treated for 6 days using our germinating seed 1 mM JA treatment (see Methods & Materials). After transplanting to the greenhouse, the length of leaf #4 was measured every 12 hours as soon as its tip appeared in the leaf whorl. Measurements were collected until leaf #4 length was no longer increasing, usually after 10 days, on average. This was done with three different concentrations of JA (10 μM, 100 μM and 1 mM), since it was performed at the same time as the previous experiment. Consistent with our results indicating that 10 μM and 100 μM JA treatment had no effect on final leaf size, no significant effects on LER or LED were identified due to JA treatment with those two concentrations (Figure 15 A and B). Although for the 100 μM treatment, two data points appeared to indicate a reduction in steady-state growth sooner than control, this was not reliably reproducible (Figure 15B). What was clear was that germinating seeds treated with 1mM JA had a reduced steady-state LER (Figure 15C). Control plants had an average LER of 3 mm/h while JA treated plants had an average LER of 2.5 mm/h (Figure 15C and Figure 16). To better visualize how leaf length (the initial measurements taken to calculate the growth rate) was affected during this period of steady-state growth, the lengths of leaf #4 were graphed at each time point along with the growth rate (Figure 16). Average leaf length was significantly lower in JA-treated plants all throughout the period of leaf #4 growth (Figure 16). Together these data suggest that the

reduction in final leaf size after a 6-day 1 mM JA treatment was due to a reduction in LER rather than LED.

Validation of Exogenous JA Treatment Effects using JA Biosynthetic Mutants

To validate my results indicating that the transient, germinating seed JA treatment can reduce LER and thus leaf size, leaf size and growth rates were measured in a JA-deficient maize mutant. I hypothesized that if increased JA content led to reduced growth rate and leaf size, then reduced JA content could increase growth rate and leaf size. To test this idea, I used a double mutant line with diminished JA content due to the loss of function mutations in two key JA biosynthesis genes: *OPR7* and *OPR8* (Y. Yan et al., 2012). 12-OXO-PHYTODIENOIC ACID REDUCTASE (OPR) is a key enzyme in the JA biosynthetic pathway responsible for converting OPDA into (+)-7-iso-JA, which is later modified into bioactive JA (Y. Yan et al., 2012). In maize, this enzyme is primarily encoded by two duplicate genes, *opr7* and *opr8,* with largely overlapping functions. Phenotypic analysis of the *opr7, opr8* double mutant line revealed that JA deficiency produced a feminized tassel, and increased blade length of leaves #1 and #2 (Figure 17A) (Y. Yan et al., 2012; Yuanxin Yan et al., 2014). Hormone profiles of the *opr7, opr8* double mutant revealed greatly reduced endogenous JA levels (Y. Yan et al., 2012).

Although leaves #1 and #2 of the *opr7, opr8* double mutant were longer, the effects of JA deficiency on growth rate in maize had not been quantified (Figure 18). To answer this question and expand on previous results, I determined LER and the final leaf size of seedling leaves #1 to #4 on seedlings from a population fixed for the recessive *opr7* mutant allele and segregating 1:2:1 for the recessive *opr8* mutant allele (+/+:*opr8*/+:*opr8/8*). Thus, this population segregates for JA deficiency like a single recessive trait. Final leaf sizes of “WT” JA sufficient genotypes, *opr7/7,* +/+ and *opr7/7,* opr8/+, were not significantly different than each other (Figure 18). In contrast, the JA deficient genotype *opr7, opr8* double mutant plants had significantly longer sheath and blade lengths compared to the WT genotypes (Figure 18). Increases in sheath length ranged from 12-40% while leaf blade length increased 12-50% (Table 4). These differences were maintained for leaves #1 - #3 for sheath length and for leaves #1 - #4 for blade length. Leaf #1 blade width of the *opr7, opr8* double mutant was significantly reduced compared to the other genotypic classes. However, as leaf number increased, leaf width of the double mutant genotype increased until it was significantly greater than leaf width of the JA sufficient genotypes

for leaves #3 and #4 (Figure 17B). An inverse relationship between leaf length and width in the JA deficient *opr7, opr8* mutant can be seen through a closer examination of percent differences comparing the double mutant to JA sufficient genotypes (Table 4). With increasing leaf number, the percent increase of leaf length diminishes (Figure 17B).

To better understand what growth processes created the increased leaf size, I determined the LER and LED within the same *opr7, opr8* segregating population. LER was significantly higher in the *opr7, opr8* double mutant genotype compared to the other genotypes, which was reflected in the length of leaf #4 being significantly longer throughout the period of growth (Figure 19). In comparison to the exogenous JA treatments, where application of JA resulted in reduced LERs and leaf size, reduced levels of endogenous JA in the *opr7, opr8* mutant increased LER and final leaf size.

Objective 1 Materials and Methods

Surface Sterilization and Seed Imbibition

For each experiment, an average of sixty to one-hundred seeds were surface sterilized for 20 minutes in 20% bleach with a drop of a surfactant (TritonX) in 50 mL conical tubes with constant inversion. Seeds were rinsed with autoclaved dH_2O five times and imbibed overnight in sterile water with shaking (orbital rocker, 80 rpm) on the benchtop at room temperature.

Standard Germinating Seed Hormone Treatment

100 mg of JA (Sigma-Aldrich) was dissolved in 3 mL of 200-proof ethanol and 44.5 mL of ddH_20 to make a stock concentration of 10 mM JA. The stock solution was stored at -80°C in 15 mL tubes. The working treatment solution was made the day treatments started by diluting the 10 mM stock with ddH_2O to a final volume of 2.5 mL/petri dish. A control solution was made by adding 3 mL of 200 proof ethanol to 44.5 mL of ddH_20 and stored at -80°C. Surface sterilized seeds imbibed overnight were placed embryo-face down, about 20 seeds/petri dish, onto a sterile paper towel and soaked with 2.5 mL of 1 mM JA in a 15 mm petri dish. Typically, three biological replicates were done per treatment, using 20 seeds/petri dish X 3 = 60 total seeds/treatment. The edges of the petri dish were sealed with parafilm to prevent evaporation and the entire petri dish was wrapped in foil and placed in a lab drawer for six days. JA treatments were placed in separate drawers than control treatments. After six days of treatment, germinated seedlings were removed from the petri dish, rinsed with sterile tap water, and transplanted to 1 gallon pots (Sunshine Mix #4 media, supplemented with 2 teaspoons osmocote, 2 teaspoon ironite) and placed in the Pope greenhouse.

JA Dose Response Treatments

B73 seeds were surface sterilized (see above) and imbibed overnight. 1 mM, 100 µM, and 10 µM JA and control solutions were made from the respective 10 mM stock. $N \geq 5$ for each treatment group (group = petri dish). Seeds were treated for six days, rinsed, and transplanted to the greenhouse, as described above. Each concentration of JA had its own matching control. Final measurements were taken when leaf #4 had stopped growing.

Exogenous JA Time Course

B73 seeds were surface sterilized (see above) and imbibed overnight. Seeds were treated with 1 mM JA or its matching control for 1, 6, 12, 24, or 48 hours in petri dishes. N ≥ 14 for each treatment group. Following treatment, seeds were rinsed with sterile tap water and transplanted to 1 gallon pots (Sunshine Mix #4 media, supplemented with 2 teaspoons osmocote, 2 teaspoon ironite). Final leaf size measurements were taken when leaf #4 had stopped growing.

Final Leaf Size Measurements

Treated seedlings were grown until the fifth leaf was completely collared (the auricle and ligule that defines the junction between the leaf sheath and blade was visible), ensuring that leaves #1 to #4 had completed growth. Sheath length, blade length, and blade width were measured for leaves #1 (most basal, first formed) to leaf #4. Leaves were measured by harvesting each leaf at its insertion into the stem. For sheath length, length was measured from the base of the sheath to the point at which the sheath transitions to the auricle at the midline of the leaf. For blade length, the length was measured along the midrib from the auricle to the distal blade tip. For blade width, width was measured at the midpoint of blade length across the blade from margin to margin.

Growth Rate Measurement

To determine LER and LED, the length of leaf #4 was measured as the distance from the insertion point of leaf #1 at the base of the plant to the tip of leaf #4. Leaf #4 length (cm) measurements began as soon as its tip was visible within the whorl and were done every 12 or 24 hours until leaf #4 stopped growing (leaf length did not change for 2-3 consecutive time points). LER was calculated by dividing the change in leaf length by the time elapsed. All LERs were converted into mm/h. LERs and leaf lengths were plotted using Microsoft Excel. A student's t-test was used to compare leaf length (cm) and LER (mm/h) at each time point.

Statistical Analysis

Significant differences were calculated in R (R Core Team, 2013). Packages used included "ggplot2", "zoo", and "multcomp". The code is available in Appendix I.

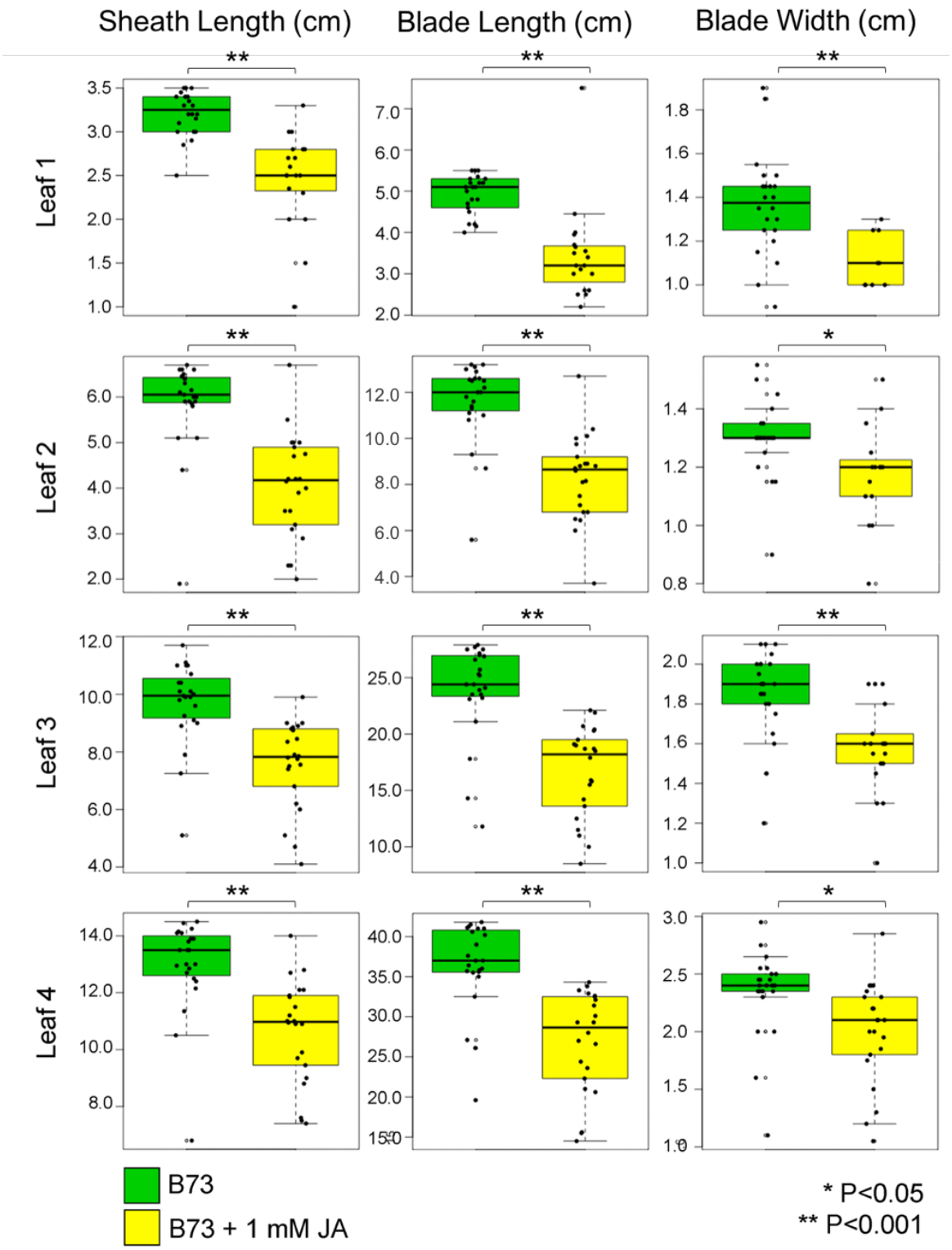

Figure 11. B73 treated with 1 mM JA shows a reduction in leaf size. Boxplots of leaves #1 to #4 following 6-day 1 mM JA treatment. Each dot is a leaf and horizontal bars represent the maximum, third quantile, median, first quantile, and minimum values respectively; dots outside of the plot are outliers. Note the change in scales on the y-axis.

Table 2. Percent reduction in final leaf size. Percent reduction was calculated using the formula [(JA-C)/C *100] where JA and C are the sheath length, blade length, and blade width by leaf number for the JA treatment (JA) and control (C). Red indicates p-value ≤ 0.05.

6 Day 1 mM JA Treatment				
	Leaf 1	**Leaf 2**	**Leaf 3**	**Leaf 4**
Sheath Length	-23.3%	-30.9%	-21.9%	-17.8%
Blade Length	-29.9%	-28.7%	-30.5%	-26.0%
Blade Width	-18.7%	-9.3%	-15.3%	-14.3%

Figure 12. B73 mature seedling leaves following a germinating seed JA treatment. Leaves #1 to #4 of 1 mM JA treated (+JA) and control (C) treated B73 seedlings. Scale bar is 5 cm.

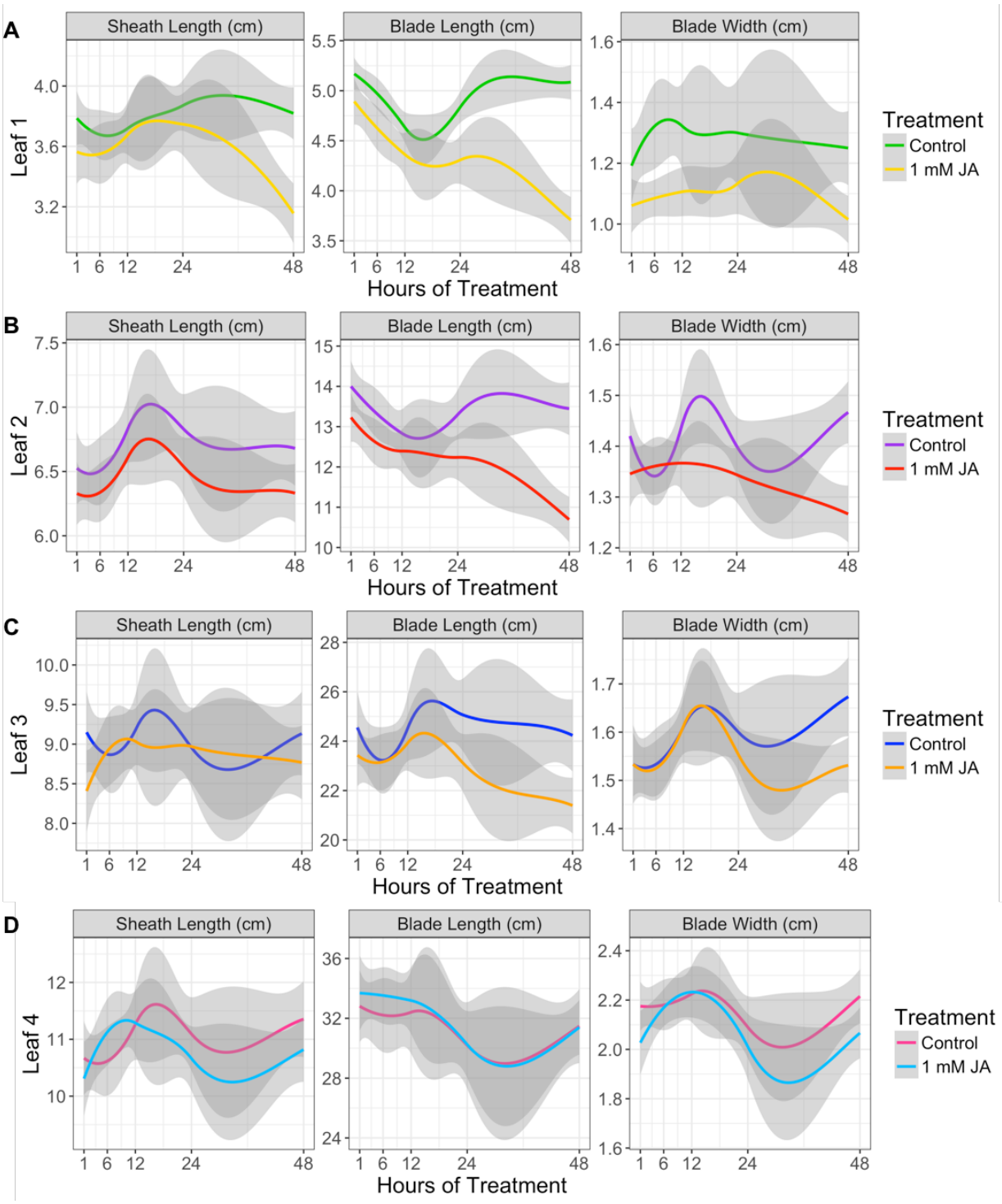

Figure 13. Effects of different JA treatment lengths on leaf size. Final leaf measurements of B73 treated with 1 mM JA or control solution for 1, 6, 12, 24, or 48 hours. Leaf #1 (A), leaf #2 (B), leaf #3 (C), and leaf #4 (D) were measured for all plants after leaf #4 was done growing. Each dot is plant, lines are smoothed conditional means, and shaded area is the 95% confidence interval. Treatments are significantly different where confidence intervals do not overlap.

Table 3. Percent differences in leaf size after 48 hours of JA treatment. Average percent differences were calculated as in Table 2. Red indicates a p-value ≤ 0.05.

48 Hour 1 mM JA Treatment				
	Leaf #1	**Leaf #2**	**Leaf #3**	**Leaf #4**
Sheath Length	-17.3%	-5.2%	-4.0%	-4.7%
Blade Length	-27.1%	-20.5%	-11.7%	-0.3%
Blade Width	-18.8%	-13.6%	-8.5%	-6.7%

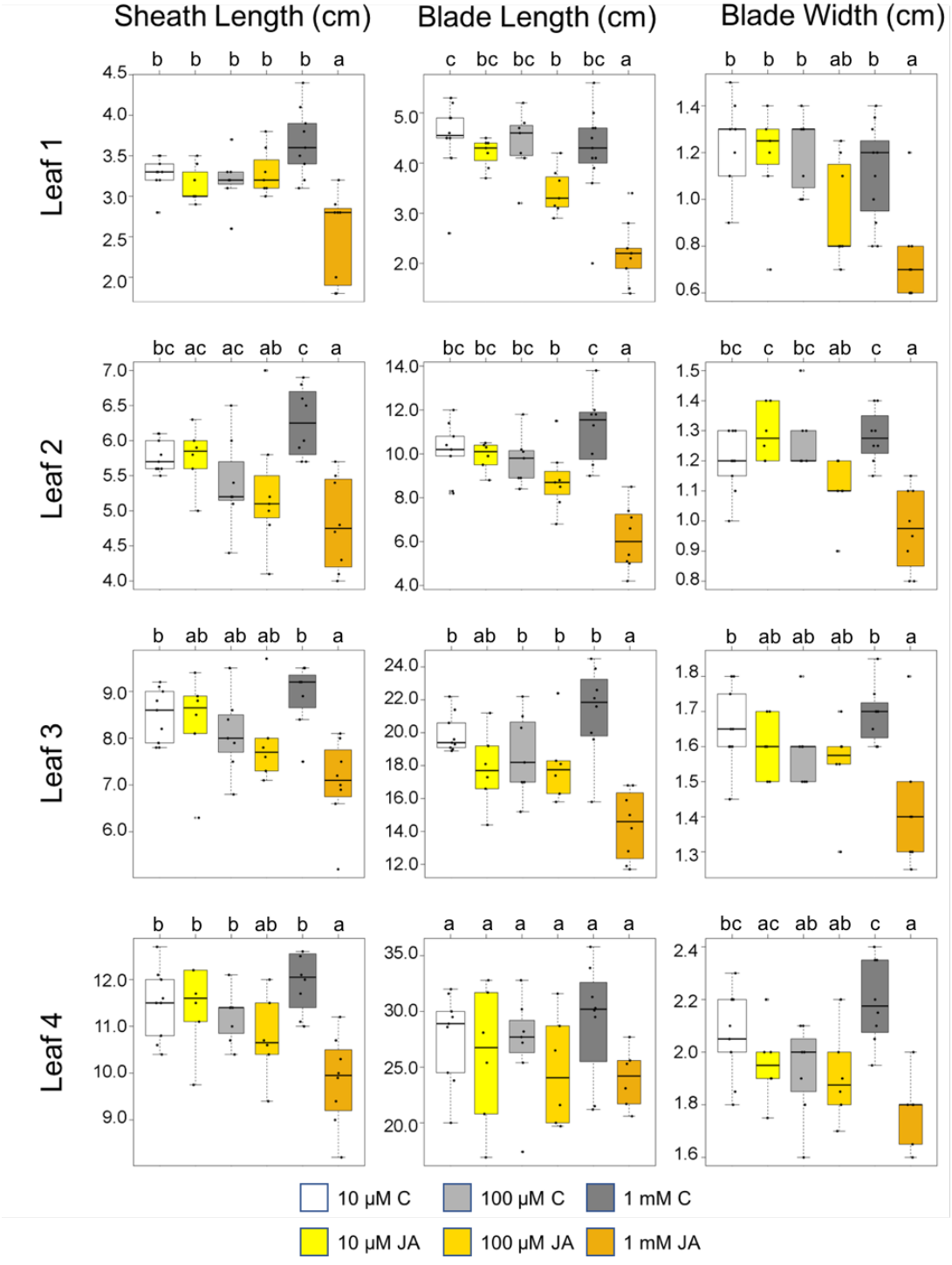

Figure 14. JA dose dependent changes in leaf size. Sheath length, blade length, and blade width measurements of (A) Leaf #1, (B) Leaf #2, (C) Leaf #3, and (D) Leaf #4 after a 6-day germinating seed treatment using 10 µM, 100 µM, or 1 mM jasmonic acid (JA) or control (C). Each dot is a leaf and horizontal bars represent the maximum, third quantile, median, first quantile, and minimum values respectively; dots outside of the plot are outliers. Groups that share a letter are not significantly different from each other.

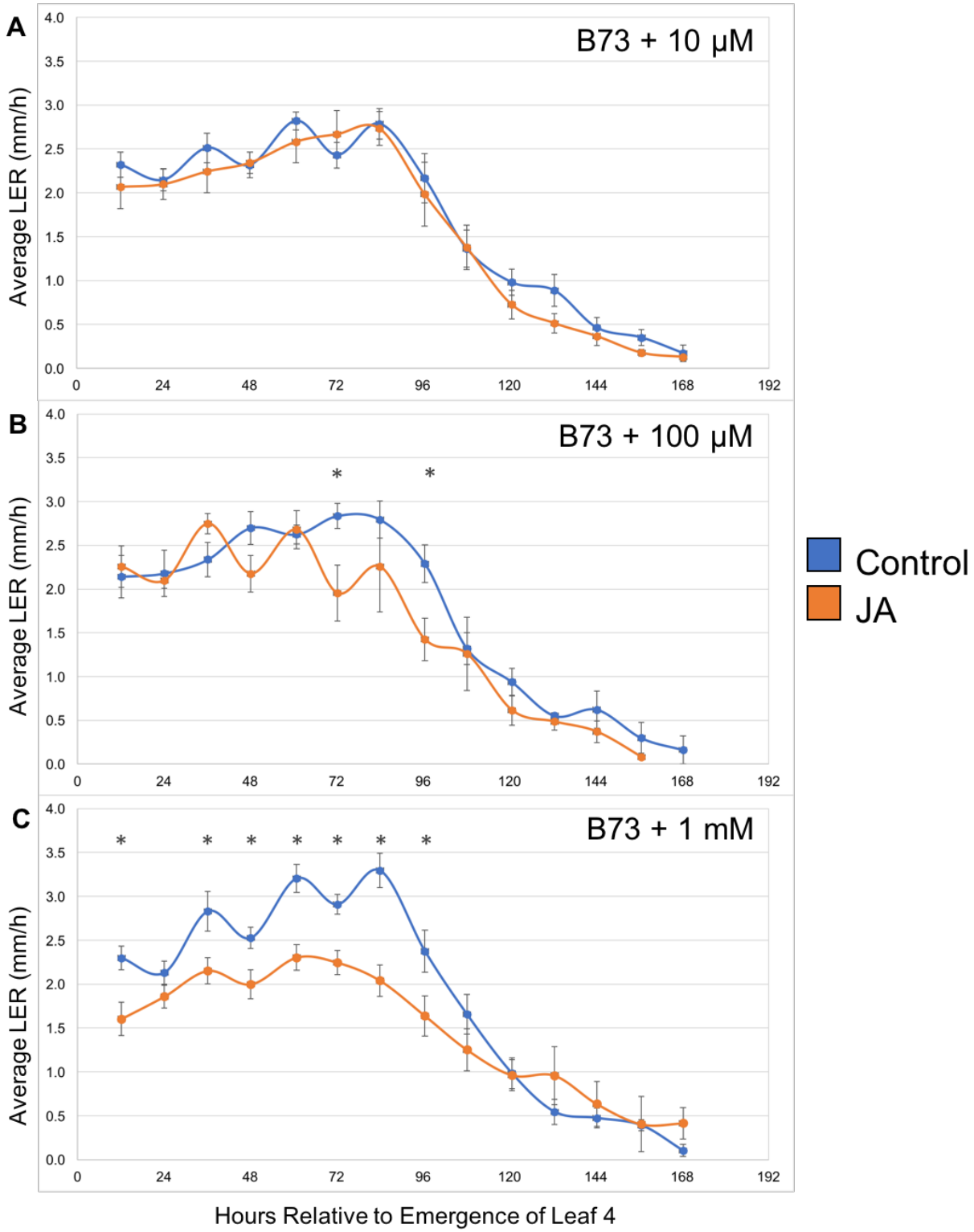

Figure 15. Response of Leaf Elongation Rate to different concentrations of JA treatment. The LER of leaf #4 LERs B73 seedlings from germinating seeds treated with (A) 10 µM, (B) 100 µM, and (C) 1 mM JA for 6 days. Significant differences by Student's t-test are marked by asterisks ($p \leq 0.05$) and error bars are SE.

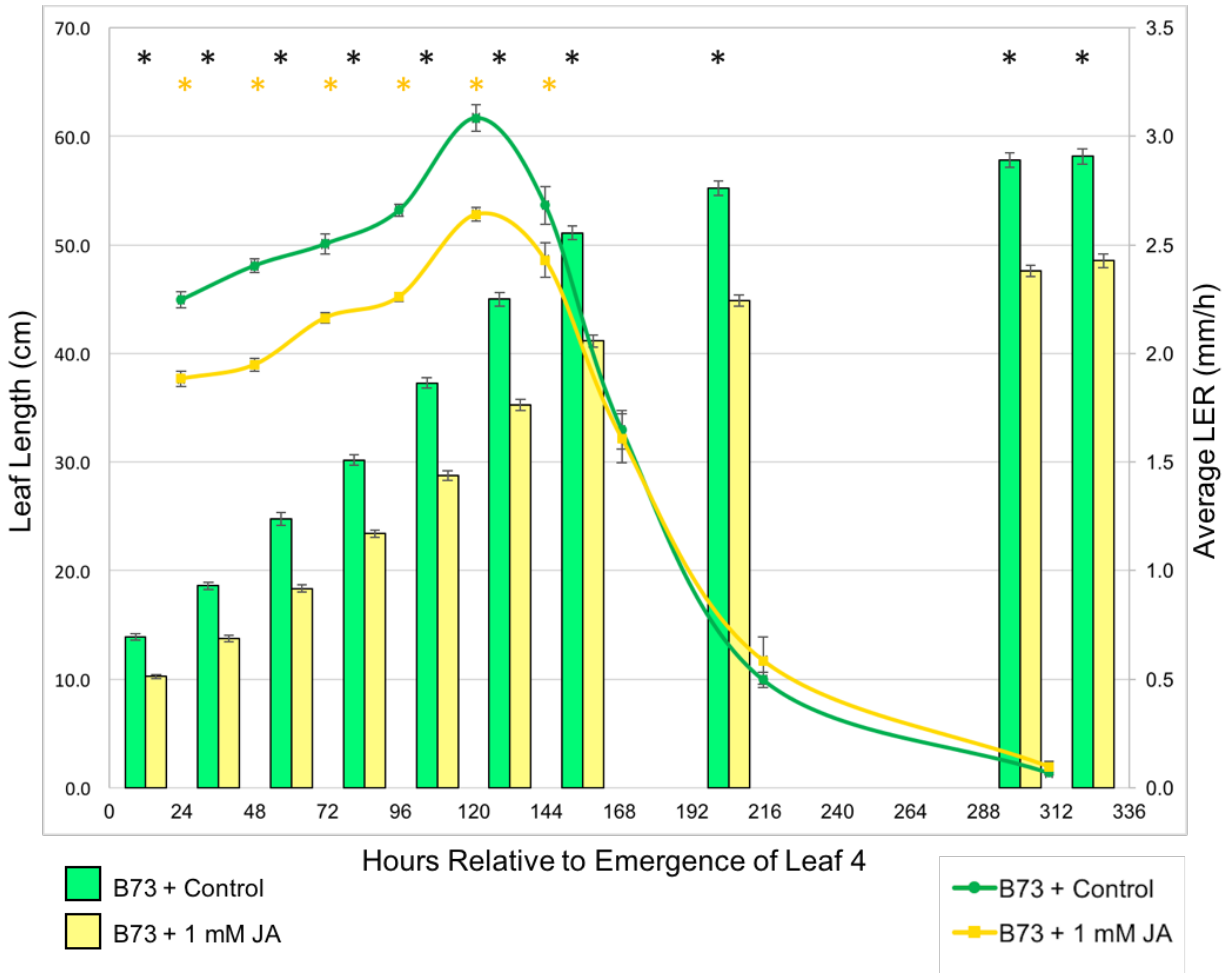

Figure 16. Comparison of leaf elongation rate and leaf length after JA treatment. Significant differences in LER are marked by yellow asterisks ($p \leq 0.05$). Significant differences in total leaf lengths are marked by black asterisks ($p \leq 0.05$). Error bars are standard error.

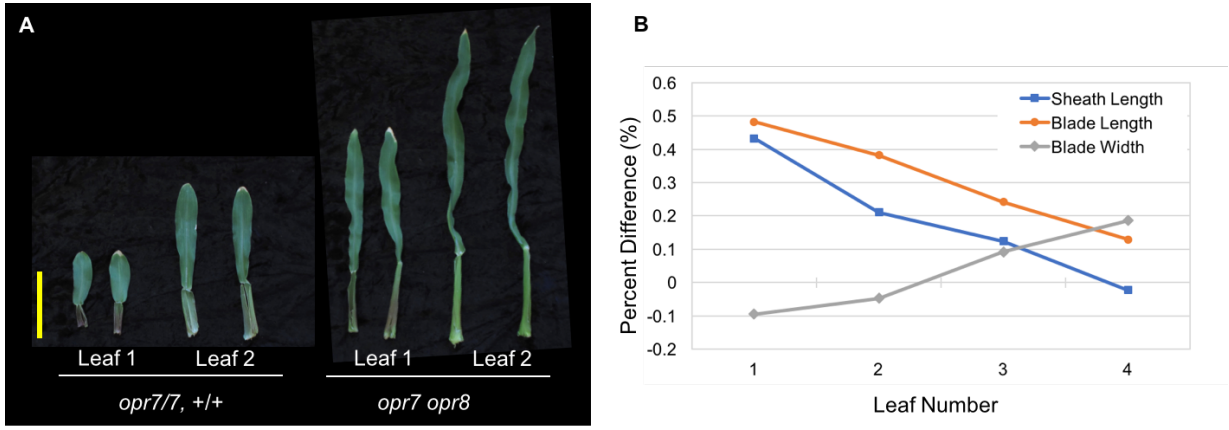

Figure 17. The JA deficient *opr7, opr8* double mutant has longer, narrower leaves than WT. (A) Representative leaf #1 and #2 of the *opr7, opr8* double mutant compared with *opr7/7, +/+* "WT". Scale bar is 5 cm. (B) Percent difference of JA deficient mutant compared to JA sufficient genotypes of sheath length, blade length, and blade width for seedling leaves #1 to #4.

Table 4. Percent difference in leaf size due to JA deficiency. Leaf size differences for the *opr7, opr8* double mutant compared to (i) the JA sufficient *opr7/7, +/+* genotype, and (ii) the *opr7/7, opr8/+* genotype. Red indicates p-value ≤ 0.05.

i.	***opr7, opr8* vs. *opr7, +/+***			
	Leaf 1	**Leaf 2**	**Leaf 3**	**Leaf 4**
Sheath Length	43.3%	21.0%	12.4%	-2.3%
Blade Length	48.2%	38.2%	24.2%	12.9%
Blade Width	-9.5%	-4.8%	9.2%	18.6%
ii.	***opr7, opr8* vs. *opr7, opr8/+***			
	Leaf 1	**Leaf 2**	**Leaf 3**	**Leaf 4**
Sheath Length	39.5%	22.2%	11.0%	-1.4%
Blade Length	43.0%	36.8%	22.6%	14.2%
Blade Width	-7.6%	-1.6%	10.0%	17.6%

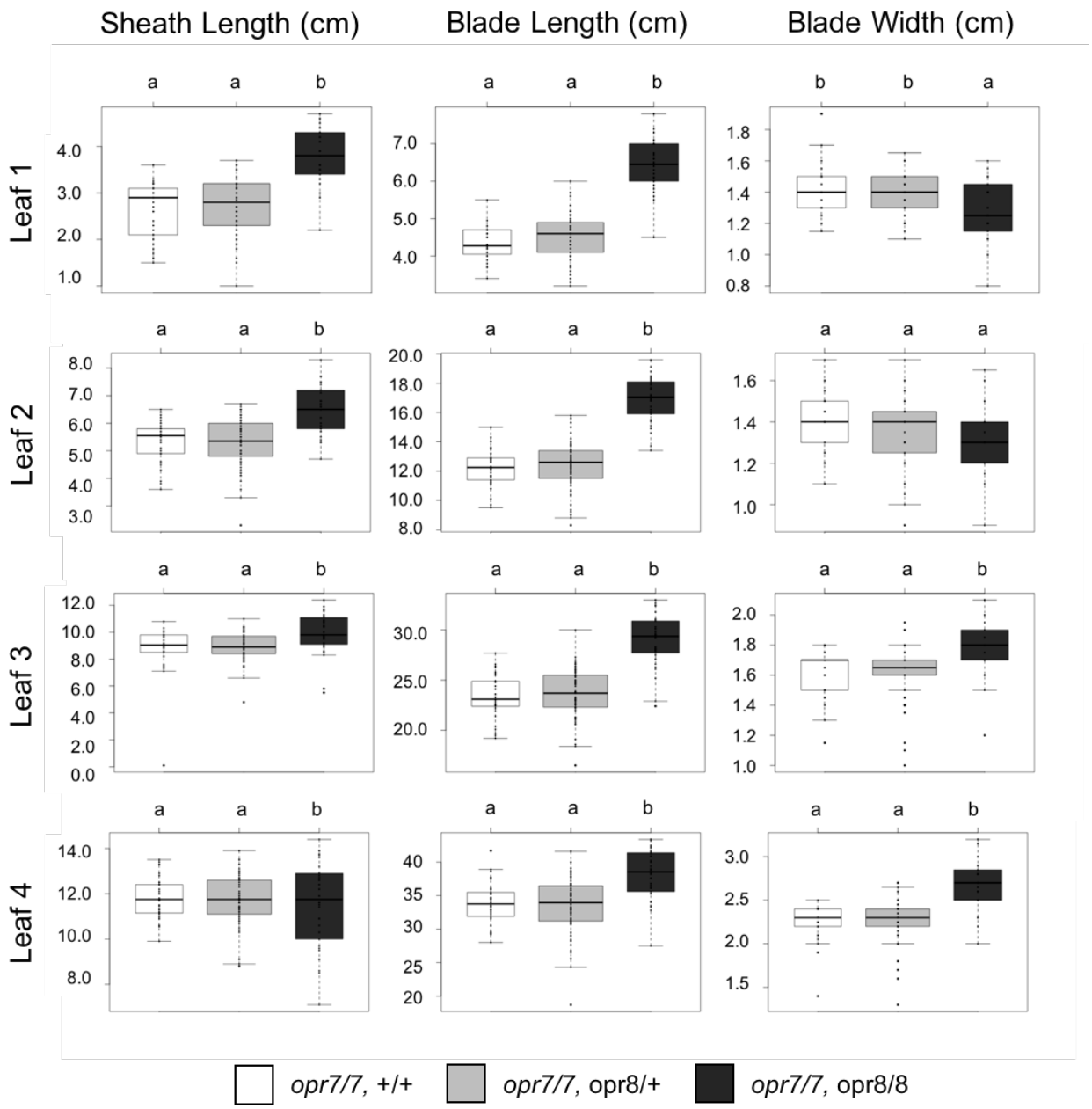

Figure 18. Comparison of leaf lengths from JA-sufficient and JA-deficient genotypes. The *opr7/7, +/+* and *opr7/7, opr8/+* genotypes are JA-sufficient and the *opr7/7, opr8/8* genotype is JA-deficient. Each dot is a leaf and horizontal bars represent the maximum, third quantile, median, first quantile, and minimum values respectively; dots outside of the plot are outliers. Groups that share a letter are not significantly different from each other.

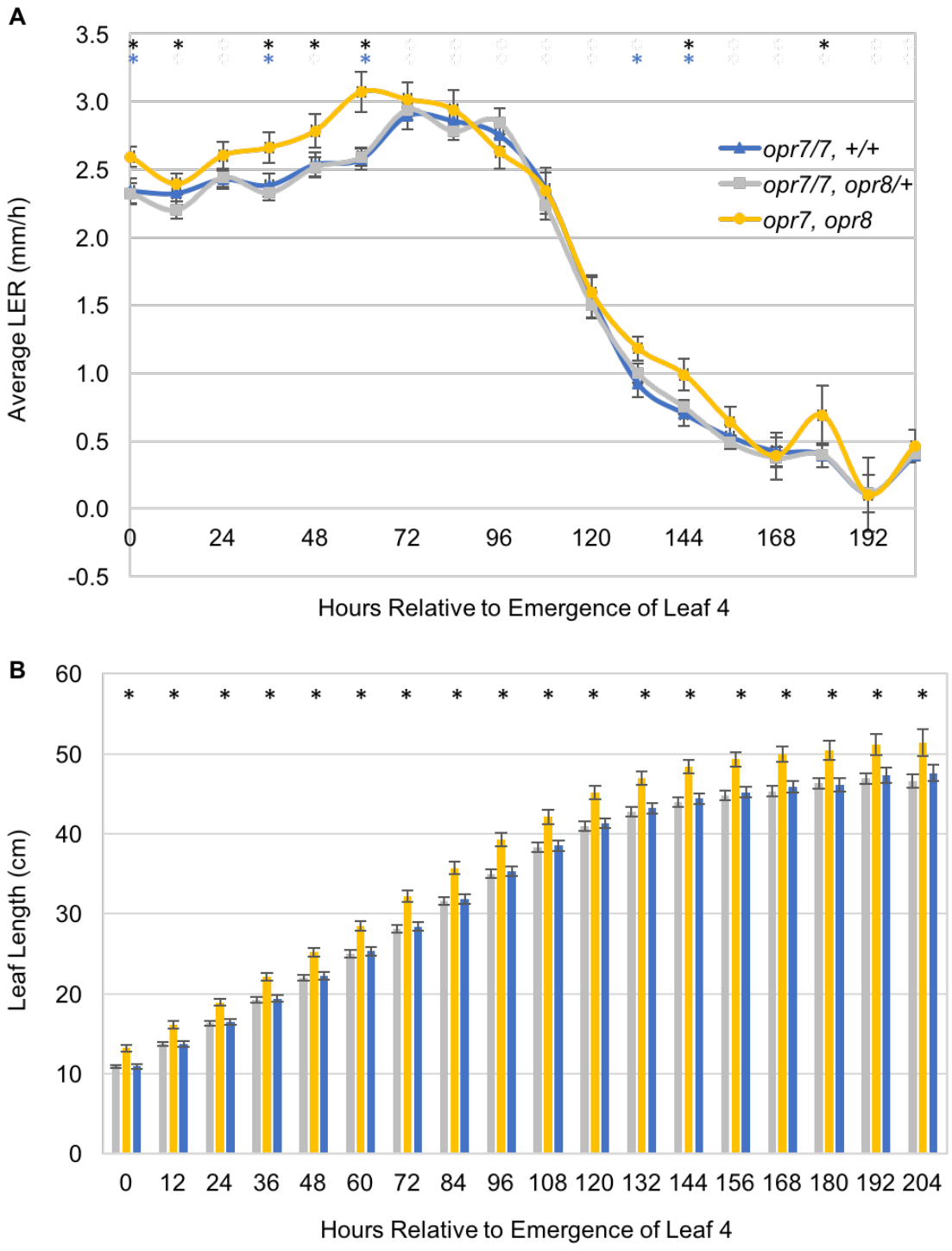

Figure 19. LER and leaf lengths of JA sufficient and JA deficient genotypes. (A) LER of the JA deficient *opr7, opr8* double mutant compared to JA sufficient *opr7/7, opr8/+* (red asterisks) and *opr7/7, +/+* (black asterisks) genotypes. Asterisks indicate significant difference p-value ≤ 0.05. (B) Leaf lengths of the three genotypes in (A). Error bars are standard error and black asterisks mark significant difference of the *opr7, opr8* mutant compared to other genotypes ($p \leq 0.05$). Color key for genotypes is the same as (A).

OBJECTIVE 2: DETERMINE THE CELLULAR CHANGES IN THE MAIZE LEAF GROWTH ZONE DUE TO EXOGENOUS JA TREATMENT

Leaf growth in maize is the result of cellular divisions and expansions that occur at the base of the leaf. We showed that JA decreased seedling leaf size and reduced steady state growth LER of normal maize inbred B73. However, we did not know how growth was changed at the cellular level by JA treatment. To determine how JA treatment affect final cellular parameters in a mature leaf, cell size, cell density and cell numbers were analyzed. Using leaf #1 from B73 seedlings that were subjected to the standard germinating seed JA treatment and control plants, glue impressions of the abaxial leaf surface were made onto a glass slide. The dried glue creates a detailed reverse image of all the epidermal cellular features from JA treated and control leaves (Figures 20 and 21). Using these glue impressions, the number of cells along a cell file from the base of the blade to the tip were counted and a cell density (# cells/cm) was calculated (Figure 20). Neither the cell length (Table 5) nor the cell density between JA-treated and control leaves were found to be significantly different (Table 5). Given that JA-treated leaves were shorter than control leaves, it was not surprising then that the total number of cells along the proximal-distal axis was significantly smaller than control (Table 5). Thus, JA treatment reduced cell number.

To measure the division zone size at steady-state growth, a partial kinematic analysis was optimized for the lab modified from Nelissen et al. (Nelissen et al., 2013). Using the germinating seedling JA treatment, leaf #4 was harvested from each treatment when just visible from the whorl until the leaf was done growing. Leaves were fixed and stained with propidium iodide, a fluorescent intercalating chemical that allows visualization of mitotic events along with some cell wall features. Using this protocol, the division zone of leaf #4 will be measured at steady state growth to see how JA changes the growth zones in future experiments (Figure 21).

Objective 2 Materials and Methods

Glue Impressions

Glue impressions were made for mature leaf #1 blade tissue from 1 mM JA-treated and control leaves. The blade of leaf #1 was dissected by cutting the sheath at the blade-sheath boundary and removing the midrib. The abaxial side of the blade was used to make the glue impression. A thin line of liquid superglue (Loctite Super Glue Ultra Liquid Control) was placed onto a clean microscope slide and the leaf blade was gently pressed onto the slide. The slide was turned upside down for about 30 minutes or until glue became opaque onto an autoclave bag or surf wax so that the glue imprint dried flat. Leaf tissue was removed from the slide using tweezers. Glue impressions were imaged at 10X using transmitted light in an EVOS FL microscope. Images were calibrated and measured in ImageJ.

Propidium Iodide Staining

Leaf #4 from 1 mM JA-treated and control plants was harvested every twenty-four hours once the leaf tip was visible in the whorl. The basal six centimeter of each leaf was placed in 1:1 EtOH:GAA (50% EtOH, 50% Glacial Acetic Acid), and the remaining mature tissue was fixed in FAA (50% EtOH, 5% Glacial Acetic Acid (GAA), 10% formalin or 37% formaldehyde and 35% water). Samples were stained with propidium iodide (Bio Basic). Powdered PI was dissolved in ddH_20 to make a 1 mg/mL stock solution and wrapped in foil for storage at 4°C. A working stock solution of 0.1 mg/mL was also made in ddH_20 and stored at 4°C. The fixed leaf tissue was moved from the 1:1 EtOH:GAA directly to a 0.1 mg/mL solution of PI and stained for about thirty seconds. Leaves were then gently unrolled onto a glass slide where the leaf was cut in half lengthwise and the midrib removed. Samples were mounted onto a glass slide in 50% glycerol and covered with a coverslip.

Samples were visualized using an epifluorescence microscope (EVOS FL) fitted with the RFP light cube (531/40 nm excitation; 593/40 nm emission). Images were collected as TIFF files and stitched together using Photomerge® Panorama in Adobe Photoshop Elements 6.

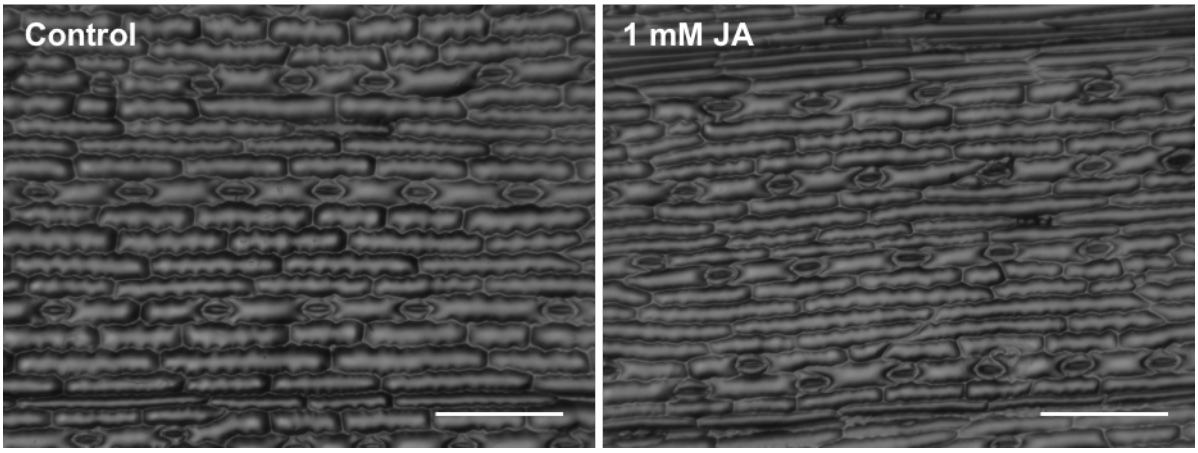

Figure 20. Cellular effects of JA treatment. Abaxial surface of B73 leaf #1 blade captured by glue impression. Scale bars are 200 µm.

Table 5. Effects of JA on cellular parameters in leaf #1. Cell density, average cell length, and number of cells was measured from abaxial glue impressions of control and JA-treated leaf #1. Red marks significant difference (Wilcoxon-Rank Sum Test, $p \leq 0.05$).

Treatment	Cell Density (cells/cm)	Average Cell Length (µm)	Number of Cells
Control	206.97 ± 2.62	153.60 ± 1.73	1047.7 ± 33.9
1 mM JA	235.54 ± 12.75	159.25 ± 2.67	534.0 ± 28.5

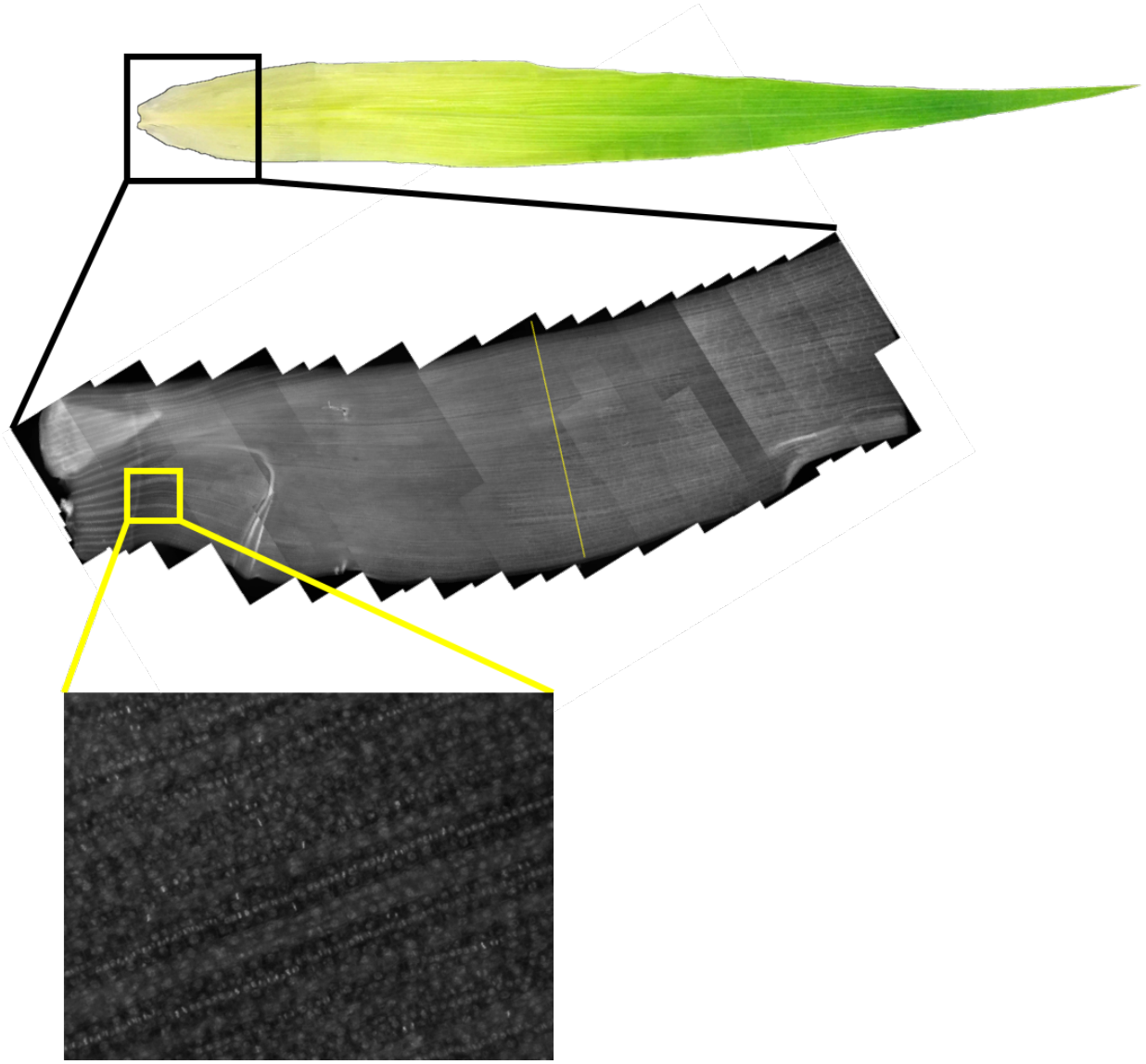

Figure 21. Visualization of leaf #4 division zone. (A) Leaf #4 of control and JA-treated B73 was fixed and stained with propidium iodide. (B) Photos were stitched together to identify the division zone. (C) Closer examination of stitched photos identifies mitotic cells

OBJECTIVE 3: DETERMINE THE EFFECTS OF EXOGENOUS JA APPLICATION ON MAIZE LEAF GROWTH IN THE HSF1 MUTANT.

Hsf1/+ *is less sensitive to JA treatment*

To elucidate the role of JA in growth suppression of the *Hsf1* mutant, seeds segregating *Hsf1*/+ and WT (+/+) in equal frequencies (1:1) were germinated in JA to determine how higher levels of exogenous JA affected leaf growth in a mutant with high endogenous levels of JA. Seeds segregating *Hsf1-1603*/+ and WT were germinated in 1 mM JA for 6 days using the standard germinating seed hormone treatment. Since two genotypes segregated in each seed treatment, there were a total of four treatment groups: WT-sibling with and without JA, and *Hsf1/*+ with and without JA. Genotypes were determined after seedlings were transplanted to the greenhouse by the presence of larger and more abundant macrohairs on the sheath of seedling leaf #1 (Figure 6B). The excessive pubescence phenotype was not affected by JA treatment and was 100% concordant with previous molecular genotype (data not shown) and thus was a reliable and reproducible method to score seedlings as either *Hsf1*/+ or WT. Previous unpublished data showed that *Hsf1*+ plant and leaf size is reduced compared to WT-siblings. Our data comparing untreated WT to *Hsf1/*+, confirmed that overall, *Hsf1*/+ leaf size was reduced compared to WT (Figure 22). With JA treatment, leaf size in both WT-sibling and *Hsf1/*+ leaf size was reduced when compared to their respective controls, but *Hsf1/*+ plants were less sensitive than WT to the JA treatment. JA treatment significantly reduced WT leaf sheath length, blade length, and blade width (as seen previously with B73) except for leaf #4 blade width (Figure 22L). Likewise, JA treated-*Hsf1*/+ plants showed reductions in blade length and some reduction in blade width compared to untreated *Hsf1/*+ plants (Figure 22 B, E, H, K and C and I). However, the sheath length of JA-treated *Hsf1*/+ plants was not significantly reduced (Figure 22 A, D, G, J). These results suggest that in the *Hsf1/*+ mutant, blade length but not the other leaf growth parameters are responsive to the JA treatment. To quantify differences in JA responsiveness, the percent growth reduction was determined (Table 6). Without any treatment, *Hsf1*/+ leaf size is normally reduced about 20% compared to its WT-sibling (Table 6i). However, while JA treatment reduces all parameters of leaf size in the WT-sibling by 20-40% (Table 6ii), only blade length in *Hsf1/*+ mutants was significantly reduced (20-40%) (Table 6iii). Sheath length in

JA-treated *Hsf1/+* was reduced by 8-16.5%, which was not significant (Table 6iii). Although *Hsf1/+* leaves were smaller than WT when both were treated with JA, the percent reduction between JA-treated *Hsf1/+* and WT was not as large as the percent reduction between untreated *Hsf1/+* and WT (Table 6iv). Overall, these results suggest that exogenous JA treatment did further suppress *Hsf1/+* growth but that the *Hsf1* mutant was less sensitive to JA than WT since only blade length was still responsive.

Leaf Elongation Duration of Hsf1 *Mutants is Shortened by JA Treatment*

Since JA treatment further reduced *Hsf1/+* leaf size, we measured *Hsf1/+* and WT growth rate with and without JA treatment to determine how leaves became smaller. LER and LED were determined for leaf # 4 of seedlings from 1 mM JA treated segregating *Hsf1* and WT seeds (as above). As seen previously in JA-treated B73, WT LER was significantly reduced by JA treatment, and was especially evident in the first 2.5 days of leaf #4 growth (Figure 23B). In contrast, *Hsf1/+* LER, especially during the first 2.5 days of steady-state growth, was not affected by JA treatment. Instead, LED was reduced by JA treatment of *Hsf1*/+ plants where steady-state growth began to slow starting at 3 days and continued to slow until leaf growth stopped (Figure 23C). Compared to WT, *Hsf1/+* LERs were reduced and LED extended with no JA treatment (Figure 23A, C). Recall that the growth rate of *Hsf1/+* is normally marked by a lower, but sustained LER and longer LED compared to WT (Nelissen, *et al.*, unpublished data). When comparing *Hsf1* with and without JA treatment, the distinctive *Hsf1/+* growth pattern was maintained, but the overall rate was reduced by JA treatment (Figure 23D).

To determine how changes in growth rate affected leaf length, LER was graphed with leaf length at each time point (sheath length + blade length) (Figure 24). For all plots, leaf length was significantly different throughout growth when a difference in LER existed at steady state growth. This was true for the following comparisons untreated WT and *Hsf1/+* (Figure 24A), untreated WT and JA-treated WT (Figure 24B), and treated WT and *Hsf1/+* (Figure 24D). Interestingly, in the comparison of untreated *Hsf1* and JA-treated *Hsf1*, leaf length only became significantly reduced in the JA-treatment when steady state growth slowed (the onset of the reduced LED) (Figure 24C). These results indicate that both LER and LED can affect final leaf size. However, changes in LER have a greater impact on final leaf size than LED, and in

the case of untreated *Hsf1/+,* an extended LED is not sufficient to compensate for the loss in size due to a reduction in initial LER.

Objective 3 Materials and Methods

Germinating Seed 1 mM JA Treatment of Hsf1

Surface sterilized seeds segregating 1 WT: 1 *Hsf1/+* were imbibed overnight and placed embryo-face down onto a sterile paper towel that was soaked with 2.5 mL of 1 mM JA in a 15 mm petri dish. The edges of the petri dish were sealed with parafilm to prevent evaporation and the entire petri dish was wrapped in foil and placed in a lab drawer for six days. JA treatments were placed in separate drawers than control treatments. After six days of treatment, germinated seedlings were removed from the petri dish, rinsed with sterile tap water, and transplanted into 1 gallon pots (Sunshine Mix #4 media, supplemented with 2 teaspoons osmocote, 2 teaspoon ironite) and placed in the greenhouse. Comparisons were made between genotypes (*Hsf1/+* or +/+) from within the same treatment petri dish.

Hsf1 Phenotyping

Hsf1/+ plants from JA-treated and control plates were identified by the outgrowth of abaxial macrohairs near the leaf collar after leaf #3 had emerged. Previous work in the lab had shown that phenoptying using this method is sufficient to infer genotype with 100% accuracy. A chi-square goodness of fit was used to test *Hsf1* segregation.

Statistical Analysis

Significant differences were calculated in R (R Core Team, 2013). Packages used included “zoo”, and “multcomp”. The code is available in Appendix I.

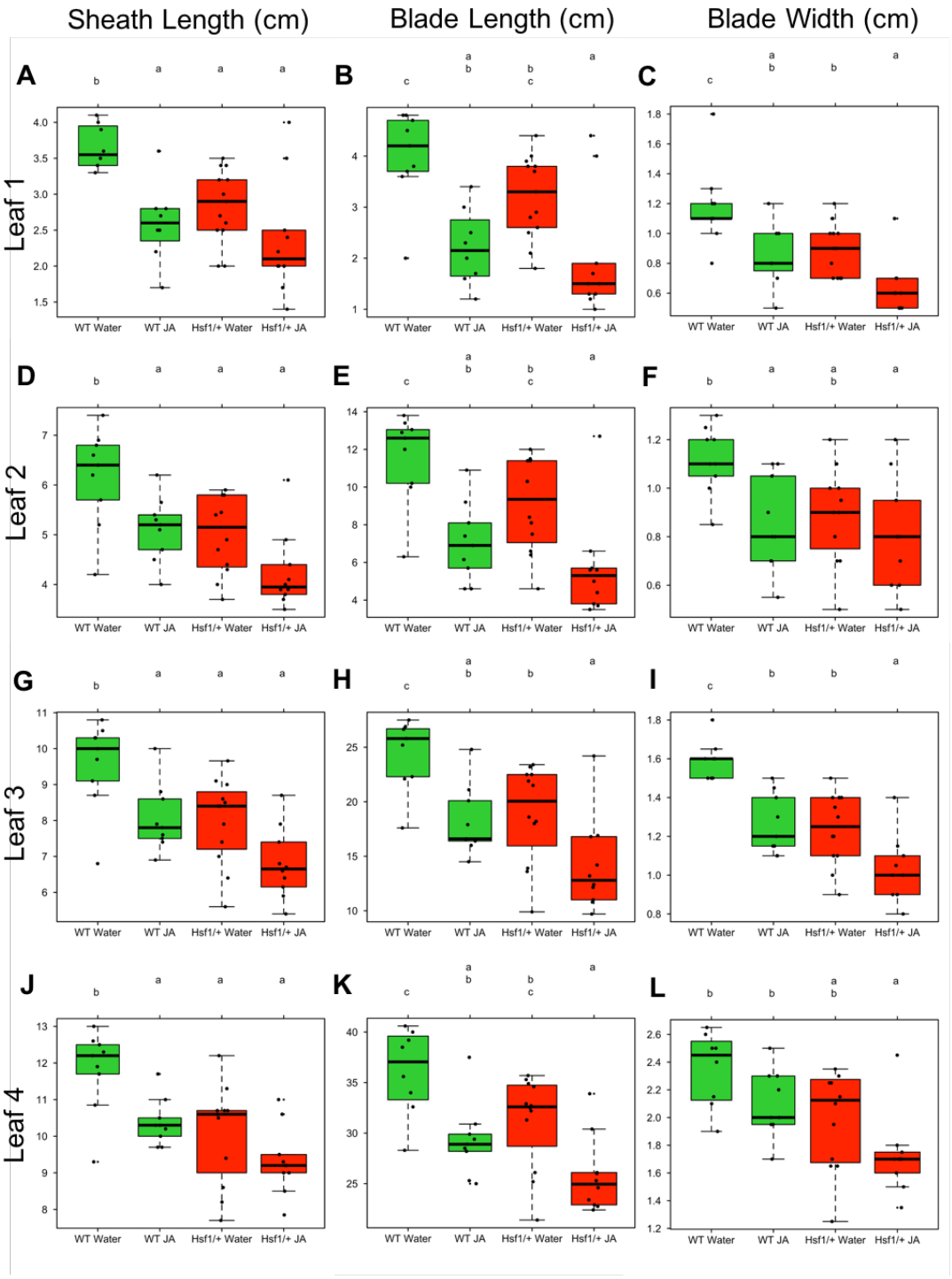

Figure 22. Final leaf sizes of *Hsf1/+* and WT-siblings treated with 1 mM JA. Boxplots of leaves #1 to #4 from seedlings grown from germinating seeds subjected to a 6-day 1 mM JA treatment. Each dot is a leaf and horizontal bars represent the maximum, third quantile, median, first quantile, and minimum values respectively; dots outside of the plot are outliers. Groups that share a letter are not significantly different.

Table 6. Relevant comparisons of percent reduction in *Hsf1/+* and WT final leaf size after JA treatment. (i) WT-sibling compared to *Hsf1/+* without JA, (ii) WT without JA compared to WT with JA treatment, (iii) *Hsf1/+* without JA compared to *Hsf1/+* with JA treatment, and (iv) WT with JA compared to *Hsf1/+* treated with JA. Red means significant percent difference $p \leq 0.05$.

i.	WT Control vs. *Hsf1/+* Control			
	Leaf 1	**Leaf 2**	**Leaf 3**	**Leaf 4**
Sheath Length	-22.2%	-18.4%	-16.5%	-14.5%
Blade Length	-20.2%	-21.9%	-22.8%	-13.5%
Blade Width	-22.9%	-20.6%	-21.8%	-15.2%

ii.	WT Control vs. WT JA			
	Leaf 1	**Leaf 2**	**Leaf 3**	**Leaf 4**
Sheath Length	-28.8%	-16.9%	-15.9%	-12.2%
Blade Length	-44.8%	-39.0%	-25.8%	-18.9%
Blade Width	-27.8%	-23.4%	-20.4%	-10.6%

iii.	*Hsf1/+* Control vs. *Hsf1/+* JA			
	Leaf 1	**Leaf 2**	**Leaf 3**	**Leaf 4**
Sheath Length	-16.5%	-15.8%	-15.0%	-7.8%
Blade Length	-38.1%	-37.4%	-25.3%	-17.5%
Blade Width	-29.0%	-9.2%	-17.6%	-13.4%

iv.	WT JA vs. *Hsf1/+* JA			
	Leaf 1	**Leaf 2**	**Leaf 3**	**Leaf 4**
Sheath Length	-8.8%	-17.3%	-15.6%	-10.2%
Blade Length	-10.5%	-19.8%	-22.4%	-12.0%
Blade Width	-24.2%	-5.9%	-19.1%	-17.9%

Figure 23. LER of JA treated *Hsf1* and WT-sib seedlings. (A) Typical growth rate pattern of WT and *Hsf1/+* is marked by an increased WT LER and a longer *Hsf1/+* LED. JA treatment (B) reduced WT LER but (C) reduced *Hsf1* LED. (D) *Hsf1* and WT-siblings maintained their growth rate pattern relative to each other even with JA treatment (D). Significant differences by Student's t-test are marked by asterisks and error bars are SE.

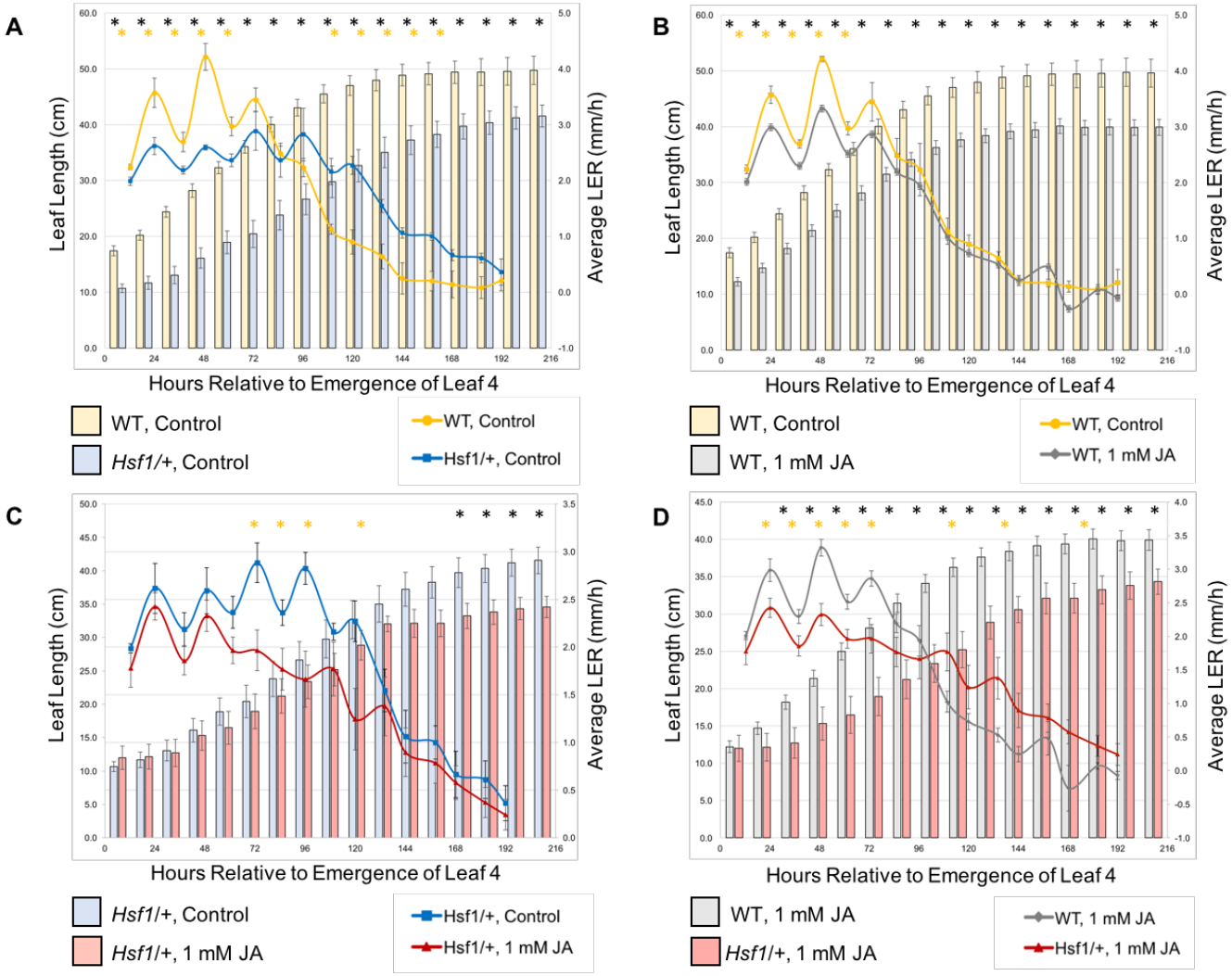

Figure 24. Average leaf elongation rate and leaf length as leaf #4 emerges in *Hsf1* and WT-sib seedlings treated with JA. (A) *Hsf1/+* control compared to WT control, (B) WT control compared to WT JA-treated, (C) comparison of *Hsf1/+* untreated and JA-treated, (D) comparison of JA-treated *Hsf1/+* and WT. Significant differences in LER are marked by yellow asterisks. Significant differences of total leaf length are marked by black asterisks. Error bars are standard error.

DISCUSSION

The reduced growth characteristics and elevated JA content in the *Hsf1* mutant suggested that CK might promote JA accumulation to modulate cellular processes for growth control. The objectives of this project were to 1) determine the growth effects of JA in maize, 2) determine the cellular effects of JA in maize, and 3) determine the effects of exogenous JA application on *Hsf1/+* leaf growth.

My results indicated that exogenous JA inhibited leaf growth and reduced JA content, in the *opr7, opr8* double mutant, increased growth. JA applied to germinating seeds reduced final size of seedling leaves #1 to #4 in the inbred B73 through a reduction in LER. When the JA concentration or treatment time were varied, I found that the growth effects of JA were time and dose dependent. A minimum germinating seed treatment time of 24 hours was sufficient to see growth effects in leaf #1 using 1 mM JA. However, a longer treatment time was necessary to see sustained growth reducing effects in leaves #1 to #3. Leaf #4 size was not affected by the germinating seed JA treatment, even after 48 hours of treatment, indicating that the minimum treatment time necessary to see a change in growth in the basal four seedling leaves is between two to six days. Leaf size response to JA was also dose dependent and final leaf size was reduced for all leaves only when treated for six days with 1 mM concentration of JA. The 10 and 100 μM concentrations of JA had no significant effects on final leaf size or growth rate. Thus, a 6-day, 1 mM JA treatment was used for my remaining experiments. Reduced growth in the maize leaf was due to reductions in LER (Figure15, 16, and 23). Analysis of leaf length during and after steady-state growth showed that JA-treated plants emerged from the whorl already shorter than the control and remained shorter throughout leaf #4 growth. This suggests that JA treated plants have differences in division zone size or differences in cell production rate prior to emergence from the whorl. Division zone differences were also suggested by the lack of change in cell size or density found in the leaf #1 epidermal cell analysis. This suggests that JA in maize affects growth similarly to *Arabidopsis* by reducing the mitotic index at the base of the leaf.

Since too much JA repressed LER and leaf size, I expected that reducing endogenous JA content should result in increased LER and larger leaves. Analysis of the JA-deficient *opr7, opr8* double mutant showed they had increased LER leading to longer leaves. Interestingly, although seedling leaves #1 to #4 were all longer in the JA mutant, the percent increase diminished with leaf number. Thus, the effect of JA

deficiency on leaf growth may primarily affect only the leaves arising in the embryo of the mature seed or juvenile leaves. These questions will need to be addressed in future studies. Although the percent increase in leaf length got smaller with increasing leaf position, the opposite was observed for leaf width. JA deficiency resulted in a narrow leaf at position #1 but led to wider leaves at positions #3 and #4 (Table 4). These data suggest that as leaf position increased the change in leaf size might be shifting from increases in length to increases in width due to JA deficiency. Thus, the regulation of leaf growth by JA might be more complex that simply increasing length, suggesting that there are more complex mechanisms partitioning growth still to be elucidated.

If the increased JA content in the *Hsf1* mutant had a direct impact on leaf size, then the *Hsf1* mutant might have a diminished response to exogenous JA. To test this idea, the CK hypersignaling *Hsf1* mutant was treated with JA. Both the *Hsf1/+* mutant and its WT-siblings responded to 1 mM exogenous JA treatment. As expected, the WT-sibling responded to JA treatment much like the B73 inbred, having smaller leaves due to a decreased LER. Interestingly, *Hsf1/+* blade length also decreased with JA treatment despite already having greater endogenous JA levels. Although *Hsf1* blade length decreased with JA application, *Hsf1/+* leaf sheath and blade width did not respond to the JA treatment. While these results show that JA perception in *Hsf1/+* is not saturated by the increased endogenous JA content, the *Hsf1* mutant is less sensitive to JA treatment. LER in the *Hsf1* mutant was also not affected by the JA treatment. Leaf length differences of JA and control *Hsf1/+* seedlings at steady state growth were largely insignificant and correlated with insignificant differences in LER. Instead, JA-treated *Hsf1* leaf elongation duration (LED) was affected, with steady state growth dropping significantly around 48 hours after the tip of leaf # 4 appeared in the whorl. This indicates JA treatment can shorten LED of *Hsf1* mutants leading to shorter leaf blade lengths. This was confirmed by the observation that leaf length only became significantly smaller than control about five days after steady state growth ended in the JA-treated *Hsf1* plants. We know from the final leaf size data that leaf lengths were different due to reduction in blade length while sheath length remained unchanged. A comparison of JA treated WT and JA treated *Hsf1/+* growth rates and leaf lengths suggested that final leaf size, at least for leaf #4 should be significantly different. This was not seen in the leaf #4 box plots (Figure 22). However, a direct comparison using a Student's t-test of the JA treatments revealed that leaf #4 sheath, blade, and width are significantly

different between JA-WT and JA-*Hsf1/+.* This discrepancy may be due to a low sample size (N>9 for each group).

In the exogenous JA treatments of both B73 and *Hsf1/+*, leaves seemed to be affected in the order of their location in the embryo. Leaf #1, the outermost leaf of the maize embryo, is the first affected, followed by leaves #2, #3, and #4. Of the three dimensions of leaf size taken in this experiment, leaf blade length exhibits the greatest sensitivity to JA treatment. Blade length was the first tissue affected in the JA time course and the tissue that experienced the greatest reduction in final size. Sheath length is the least to be affected by JA treatment. These differences in leaf tissue sensitivity might be due to: (1) JA treatment does not permeate sheath cells as they are a different type of leaf tissue; (2) JA does permeate sheath cells, but those cells are not at a physiological stage where JA will have an effect; or (3) both the timing and physiology have an effect because reduction in sheath length was observed in the 6-day, 1 mM JA treatment. Whether the insensitivity to JA treatment in *Hsf1/+* sheath tissue is due to the endogenous levels of JA remains to be discovered.

Hsf1 is the only mutant of its kind in plants. Though *Arabidopsis* has largely been used to elucidate various hormone biosynthesis, signaling, and crosstalk pathways, no CK hypersignaling mutant with elevated JA has been published. Although much of the biosynthesis and signaling components of CK and JA are conserved between monocots and dicots, the CK-JA crosstalk and the way it affects growth may not. The data presented above show that the growth reduction in *Hsf1* was not completely accounted for by JA treatment in both final leaf size and growth rate data. This suggests that other hormones are involved with the *Hsf1* growth reduction and further establishes *Hsf1* as a useful model to understand the hormonal networks guiding leaf growth. Moreover, the data presented above provide a physiological framework in which further molecular and genetic studies can be grounded to dissect the mechanism of CK-JA crosstalk.

APPENDIX

R Code

Simple Boxplots (Figure 11)

```
all<-read.csv("SA#3R.csv", header= T)
attach(all)

y=L4W
x=Treatment
levels(x)
t.test(y~x, data=all)

opar<- par(mai=c(1,1,1,1))
plot(y~x, varwidth=T, col=c("green3", "yellow"), ylab="   ", cex=0.5)
stripchart(y~x, vert=TRUE, method="jitter", las=2, pch=16, add=TRUE, cex=.8)
```

Boxplots with compact letter display (Figure 14, 18)

```
setwd(" ")
FLL<-read.csv("SA#19_fll2.csv", header =T)
attach(FLL)

library("zoo")
library("multcomp")

x=CT
x<-factor(x,levels(x)[c(3,4,1,2,5,6)])
levels(x)

y=L1S
fit<-aov(y~x, data=FLL)
summary(fit)
tuk<- glht(fit, linfct=mcp(x="Tukey"))
summary(tuk)
tuk.cld<-cld(tuk, level=0.05)
opar<- par(mai=c(.5,.9,1,.5))
plot(tuk.cld, varwidth=T, col=c("gray100", "yellow", "gray70", "gold",
"gray50","darkgoldenrod2"), ylab="L1S", cex=0.5)
stripchart(y~x, vert="T", method="jitter", las=2, pch=16, add=TRUE, cex=0.8)
dev.print(width=4, height=5, horizontal =FALSE)
dev.copy(pdf,'L1S.pdf')
dev.off()
```

Smoothed Conditional Means using LOESS (Figure 13)

```
attach(DATA)
str(DATA)
library(ggplot2)
levels(Tissue)
levels(Treatment)
levels(DATA$Tissue)<-c("Blade Length (cm)", "Sheath Length (cm)", "Blade Width (cm)")
DATA$Tissue<-factor(DATA$Tissue, levels(DATA$Tissue)[c(2,1,3)])
levels(DATA$Tissue)
levels(DATA$Treatment)<-c("Control", "1 mM JA")
```

```
attach(DATA)
L1<-subset(DATA, LeafNumber=="L1")
L2<-subset(DATA, LeafNumber=="L2")
L3<-subset(DATA, LeafNumber=="L3")
L4<-subset(DATA, LeafNumber=="L4")

mycol<-c("green3", "gold1")
p<-ggplot(L1, aes(Hours, Measure, col=Treatment))
p+geom_smooth(model="loess", size=1) +
  facet_wrap(~ Tissue, scale="free") +
  theme_bw() +
  theme(text=element_text(size=16))+
  scale_color_manual(values=mycol) +
  ylab("Measurement (cm)") +
  xlab("Hours of Treatment") +
  scale_x_continuous(name="Hours of Treatment", breaks=c(1,6,12,24,48))+
  scale_y_continuous(name="Leaf 1")
ggsave("L1Time_s_nj.png", width=10, height=3)

L2col<-c("purple", "red")
p<-ggplot(L2, aes(Hours, Measure, col=Treatment))
p+geom_smooth(model="loess", size=1) +
  facet_wrap(~ Tissue, scale="free") +
  theme_bw() +
  theme(text=element_text(size=16))+
  scale_color_manual(values=L2col) +
  ylab("Measurement (cm)") +
  xlab("Hours of Treatment") +
  scale_x_continuous(name="Hours of Treatment", breaks=c(1,6,12,24,48))+
  scale_y_continuous(name="Leaf 2")
ggsave("L2Time_s_nj.png", width=10, height=3)

L3col<-c("blue", "orange")
p<-ggplot(L3, aes(Hours, Measure, col=Treatment))
p+geom_smooth(model="loess", size=1) +
  facet_wrap(~ Tissue, scale="free") +
  theme_bw() +
  theme(text=element_text(size=16))+
  scale_color_manual(values=L3col) +
  ylab("Measurement (cm)") +
  xlab("Hours of Treatment") +
  scale_x_continuous(name="Hours of Treatment", breaks=c(1,6,12,24,48))+
  scale_y_continuous(name="Leaf 3")
ggsave("L3Time_s_nj.png", width=10, height=3)

L4col<-c("violetred1", "deepskyblue")
p<-ggplot(L4, aes(Hours, Measure, col=Treatment))
p+geom_smooth(model="loess", size=1) +
  facet_wrap(~ Tissue, scales="free") +
  theme_bw() +
  theme(text=element_text(size=16))+
  scale_color_manual(values=L4col) +
  ylab("Measurement (cm)") +
  xlab("Hours of Treatment") +
  scale_x_continuous(name="Hours of Treatment", breaks=c(1,6,12,24,48))+
  scale_y_continuous(name="Leaf 4")
ggsave("L4Time_s_nj.png", width=10, height=3)
```

Hsf1/+ Box Plots (Figure 22)

```
all<-read.csv("SA#12all.csv", header=T)

all<-data.frame(all)
attach(all)

y= L1S
x= GenTreat
levels(x)
x<-factor(x,levels(x)[c(3,4,1,2)])
levels(x)

ANOVA<-aov(y~x,data=all)
tuk<- glht(ANOVA, linfct=mcp(x="Tukey"))
summary(tuk)
tuk.cld<- cld(tuk, level=0.05)
opar<- par(mai=c(1,1,1,1))
plot(tuk.cld, varwidth=T, names=c("WT Water", "WT JA", "Hsf1/+ Water", "Hsf1/+ JA"),
col=c("limegreen", "limegreen", "red", "red"), ylab="L1S (cm)", cex=0.5)
stripchart(y~x, vert=TRUE, method="jitter", las=2, pch=16, add=TRUE, cex=0.8)
par(cex.lab=1.8) #y axis
par(cex.axis=1.8) #x axis
dev.copy(png,'L1S.png')
dev.off()

y= L1B
ANOVA<-aov(y~x,data=all)
tuk<- glht(ANOVA, linfct=mcp(x="Tukey"))
summary(tuk)
tuk.cld<- cld(tuk, level=0.05)
opar<- par(mai=c(1,1,1,1))
plot(tuk.cld, varwidth=T, names=c("WT Water", "WT JA", "Hsf1/+ Water", "Hsf1/+ JA"),
col=c("limegreen", "limegreen", "red", "red"), ylab="L1B (cm)", cex=0.5)
stripchart(y~x, vert=TRUE, method="jitter", las=2, pch=16, add=TRUE, cex=0.8)
dev.copy(png,'L1B.png')
dev.off()

y= L1W
ANOVA<-aov(y~x,data=all)
tuk<- glht(ANOVA, linfct=mcp(x="Tukey"))
summary(tuk)
tuk.cld<- cld(tuk, level=0.05)
opar<- par(mai=c(1,1,1,1))
plot(tuk.cld, varwidth=T, names=c("WT Water", "WT JA", "Hsf1/+ Water", "Hsf1/+ JA"),
col=c("limegreen", "limegreen", "red", "red"), ylab="L1W (cm)", cex=0.5)
stripchart(y~x, vert=TRUE, method="jitter", las=2, pch=16, add=TRUE, cex=0.8)
dev.copy(png,'L1W.png')
dev.off()

y= L2S
ANOVA<-aov(y~x,data=all)
tuk<- glht(ANOVA, linfct=mcp(x="Tukey"))
summary(tuk)
tuk.cld<- cld(tuk, level=0.05)
opar<- par(mai=c(1,1,1,1))
plot(tuk.cld, varwidth=T, names=c("WT Water", "WT JA", "Hsf1/+ Water", "Hsf1/+ JA"),
col=c("limegreen", "limegreen", "red", "red"), ylab="L2S (cm)", cex=0.5)
stripchart(y~x, vert=TRUE, method="jitter", las=2, pch=16, add=TRUE, cex=0.8)
dev.copy(png,'L2S.png')
dev.off()
```

```
y= L2B
ANOVA<-aov(y~x,data=all)
tuk<- glht(ANOVA, linfct=mcp(x="Tukey"))
summary(tuk)
tuk.cld<- cld(tuk, level=0.05)
opar<- par(mai=c(1,1,1,1))
plot(tuk.cld, varwidth=T, names=c("WT Water", "WT JA", "Hsf1/+ Water", "Hsf1/+ JA"),
col=c("limegreen", "limegreen", "red", "red"), ylab="L2B (cm)", cex=0.5)
stripchart(y~x, vert=TRUE, method="jitter", las=2, pch=16, add=TRUE, cex=0.8)
dev.copy(png,'L2B.png')
dev.off()

y= L2W
ANOVA<-aov(y~x,data=all)
tuk<- glht(ANOVA, linfct=mcp(x="Tukey"))
summary(tuk)
tuk.cld<- cld(tuk, level=0.05)
opar<- par(mai=c(1,1,1,1))
plot(tuk.cld, varwidth=T, names=c("WT Water", "WT JA", "Hsf1/+ Water", "Hsf1/+ JA"),
col=c("limegreen", "limegreen", "red", "red"), ylab="L2W (cm)", cex=0.5)
stripchart(y~x, vert=TRUE, method="jitter", las=2, pch=16, add=TRUE, cex=0.8)
dev.copy(png,'L2W.png')
dev.off()

y= L3S
ANOVA<-aov(y~x,data=all)
tuk<- glht(ANOVA, linfct=mcp(x="Tukey"))
summary(tuk)
tuk.cld<- cld(tuk, level=0.05)
opar<- par(mai=c(1,1,1,1))
plot(tuk.cld, varwidth=T, names=c("WT Water", "WT JA", "Hsf1/+ Water", "Hsf1/+ JA"),
col=c("limegreen", "limegreen", "red", "red"), ylab="L3S (cm)", cex=0.5)
stripchart(y~x, vert=TRUE, method="jitter", las=2, pch=16, add=TRUE, cex=0.8)
dev.copy(png,'L3S.png')
dev.off()

y= L3B
ANOVA<-aov(y~x,data=all)
tuk<- glht(ANOVA, linfct=mcp(x="Tukey"))
summary(tuk)
tuk.cld<- cld(tuk, level=0.05)
opar<- par(mai=c(1,1,1,1))
plot(tuk.cld, varwidth=T, names=c("WT Water", "WT JA", "Hsf1/+ Water", "Hsf1/+ JA"),
col=c("limegreen", "limegreen", "red", "red"), ylab="L3B (cm)", cex=0.5)
stripchart(y~x, vert=TRUE, method="jitter", las=2, pch=16, add=TRUE, cex=0.8)
dev.copy(png,'L3B.png')
dev.off()

y= L3W
ANOVA<-aov(y~x,data=all)
tuk<- glht(ANOVA, linfct=mcp(x="Tukey"))
summary(tuk)
tuk.cld<- cld(tuk, level=0.05)
opar<- par(mai=c(1,1,1,1))
plot(tuk.cld, varwidth=T, names=c("WT Water", "WT JA", "Hsf1/+ Water", "Hsf1/+ JA"),
col=c("limegreen", "limegreen", "red", "red"), ylab="L3W (cm)", cex=0.5)
stripchart(y~x, vert=TRUE, method="jitter", las=2, pch=16, add=TRUE, cex=0.8)
dev.copy(png,'L3W.png')
dev.off()
```

```
y= L4S
ANOVA<-aov(y~x,data=all)
tuk<- glht(ANOVA, linfct=mcp(x="Tukey"))
summary(tuk)
tuk.cld<- cld(tuk, level=0.05)
opar<- par(mai=c(1,1,1,1))
plot(tuk.cld, varwidth=T, names=c("WT Water", "WT JA", "Hsf1/+ Water", "Hsf1/+ JA"),
col=c("limegreen", "limegreen", "red", "red"), ylab="L4S (cm)", cex=0.5)
stripchart(y~x, vert=TRUE, method="jitter", las=2, pch=16, add=TRUE, cex=0.8)
dev.copy(png,'L4S.png')
dev.off()

y= L4B
ANOVA<-aov(y~x,data=all)
tuk<- glht(ANOVA, linfct=mcp(x="Tukey"))
summary(tuk)
tuk.cld<- cld(tuk, level=0.05)
opar<- par(mai=c(1,1,1,1))
plot(tuk.cld, varwidth=T, names=c("WT Water", "WT JA", "Hsf1/+ Water", "Hsf1/+ JA"),
col=c("limegreen", "limegreen", "red", "red"), ylab="L4B (cm)", cex=0.5)
stripchart(y~x, vert=TRUE, method="jitter", las=2, pch=16, add=TRUE, cex=0.8)
dev.copy(png,'L4B.png')
dev.off()

y= L4W
ANOVA<-aov(y~x,data=all)
tuk<- glht(ANOVA, linfct=mcp(x="Tukey"))
summary(tuk)
tuk.cld<- cld(tuk, level=0.05)
opar<- par(mai=c(1,1,1,1))
plot(tuk.cld, varwidth=T, names=c("WT Water", "WT JA", "Hsf1/+ Water", "Hsf1/+ JA"),
col=c("limegreen", "limegreen", "red", "red"), ylab="L4W (cm)", cex=0.5)
stripchart(y~x, vert=TRUE, method="jitter", las=2, pch=16, add=TRUE, cex=0.8)
dev.copy(png,'L4W.png')
dev.off()
```

WORKS CITED

Amasino, R. (2005). 955: Kinetin Arrives. The 50th Anniversary of a New Plant Hormone. *Plant Physiology*, *138*, 1177–1184. http://doi.org/10.1104/pp.104.900160

Bertrand-Garcia, R., & Freeling, M. (1991). Hairy-Sheath Frayed # 1-0 : A Systemic , Heterochronic Mutant of Maize that Specifies Slow Developmental Stage Transitions Author (s): Ralph Bertrand-Garcia and Michael Freeling Source : American Journal of Botany , Vol . 78 , No . 6 (Jun ., 1991), pp, *78*(6), 747–765.

Bishopp, A., Lehesranta, S., Vatén, A., Help, H., El-Showk, S., Scheres, B., … Helariutta, Y. (2011). Phloem-transported cytokinin regulates polar auxin transport and maintains vascular pattern in the root meristem. *Current Biology : CB*, *21*(11), 927–32. http://doi.org/10.1016/j.cub.2011.04.049

Cahill, J. (2015). *Analysis of cytokinin-induced maize leaf developmental changes and interacting genetic modifiers*. *Master's Thesis*. Iowa State University.

Campos, M. L., Yoshida, Y., Major, I. T., de Oliveira Ferreira, D., Weraduwage, S. M., Froehlich, J. E., … Wellburn, A. R. (2016). Rewiring of jasmonate and phytochrome B signalling uncouples plant growth-defense tradeoffs. *Nature Communications*, *7*, 12570. http://doi.org/10.1038/ncomms12570

Chaw, S.-M., Chang, C.-C., Chen, H.-L., & Li, W.-H. (2004). Dating the Monocot–Dicot Divergence and the Origin of Core Eudicots Using Whole Chloroplast Genomes. *Journal of Molecular Evolution*, *58*, 424–441. http://doi.org/10.1007/s00239-003-2564-9

Choi, J., Huh, S. U., Kojima, M., Sakakibara, H., Paek, K.-H., & Hwang, I. (2010). The cytokinin-activated transcription factor ARR2 promotes plant immunity via TGA3/NPR1-dependent salicylic acid signaling in Arabidopsis. *Developmental Cell*, *19*(2), 284–95. http://doi.org/10.1016/j.devcel.2010.07.011

Coley, P. D., Bryant, J. P., & Chapin III, F. S. (1985). Resource Availability and Plant Antiherbivore Defense. *Science*, *230*(4728), 895–899.

Creelman, R. A., & Mullet, J. E. (1997). Biosynthesis and Action of Jasmonates in Plants. *Annual Review of Plant Physiology and Plant Molecular Biology*, *48*, 355–381. http://doi.org/10.1146/annurev.arplant.48.1.355

De Vleesschauwer, D., Xu, J., & Hofte, M. (2014). Making sense of hormone-mediated defense networking: from rice to Arabidopsis. *Frontiers in Plant Science*, *5*(611), 1–15. http://doi.org/10.3389/fpls.2014.00611

Du, F., Guan, C., & Jiao, Y. (2018). Molecular Mechanisms of Leaf Morphogenesis. *Molecular Plant*, *0*(0). http://doi.org/10.1016/j.molp.2018.06.006

Durand, A. N., Pauwels, L., & Goossens, A. (2016). The Ubiquitin System and Jasmonate Signaling. *Plants*, *5*(1), 6. http://doi.org/10.3390/plants5010006

Engelsdorf, T., Horst, R. J., Pröls, R., Pröschel, M., Dietz, F., Hückelhoven, R., & Voll, L. M. (2013). Reduced Carbohydrate Availability Enhances the Susceptibility of Arabidopsis toward Colletotrichum higginsianum 1[W][OA]. *Plant Physiol*, *162*, 225–238. http://doi.org/10.1104/pp.112.209676

Eric Schaller, G., Street, I. H., Kieber, J. J., & Eric, G. (2014). Cytokinin and the cell cycle. *Current Opinion in Plant Biology*, *21*, 7–15. http://doi.org/10.1016/j.pbi.2014.05.015

Ferreira, F. J., & Kieber, J. J. (2005). Cytokinin signaling. *Current Opinion in Plant Biology*, *8*(5), 518–525. http://doi.org/10.1016/J.PBI.2005.07.013

Fré Bort, I., Kowalska, M., Hluska, T. Š., Fré Bortová, J., & Galuszka, P. (2011). Evolution of cytokinin biosynthesis and degradation. *Journal of Experimental Botany*, *62*(8), 2431–2452. http://doi.org/10.1093/jxb/err004

Frebort, I., Kowalska, M., Hluska, T., Frebortova, J., & Galuszka, P. (2011). Evolution of cytokinin biosynthesis and degradation. *Journal of Experimental Botany*, *62*(8), 2431–2452. http://doi.org/10.1093/jxb/err004

Han, G.-Z. (2016). Evolution of jasmonate biosynthesis and signaling mechanisms. *Journal of Experimental Botany*, *68*(6), erw470. http://doi.org/10.1093/jxb/erw470

Hou, X., Ding, L., & Yu, H. (2013). Crosstalk between GA and JA signaling mediates plant growth and defense. *Plant Cell Reports*, *32*(7), 1067–1074. http://doi.org/10.1007/s00299-013-1423-4

Huffaker, A., Pearce, G., Veyrat, N., Erb, M., Turlings, T. C. J., Sartor, R., … Schmelz, E. a. (2013). Plant elicitor peptides are conserved signals regulating direct and indirect antiherbivore defense.

Proceedings of the National Academy of Sciences of the United States of America, *110*(14), 5707–12. http://doi.org/10.1073/pnas.1214668110
Huot, B., Yao, J., Montgomery, B. L., & He, S. Y. (2014). Growth-Defense Tradeoffs in Plants: A Balancing Act to Optimize Fitness. *Molecular Plant*, *7*(8), 1267–1287. http://doi.org/10.1093/mp/ssu049
Kang, J., Lee, Y., Sakakibara, H., & Martinoia, E. (2017). Cytokinin Transporters: GO and STOP in Signaling. *Trends in Plant Science*, *22*(6), 455–461. http://doi.org/10.1016/j.tplants.2017.03.003
Kang, N. Y., Cho, C., & Kim, J. (2013). Inducible expression of Arabidopsis response regulator 22 (ARR22), a type-C ARR, in transgenic Arabidopsis enhances drought and freezing tolerance. *PloS One*, *8*(11), e79248. http://doi.org/10.1371/journal.pone.0079248
Kiesselbach, T. A. (1999). *The Structure and Reproduction of Corn*. (D. Brown & S. Schaefer, Eds.) (50th Anniv). Cold Spring Harbor, NY: Cold Spring Harbor Laboratory Press.
Ko, D., Kang, J., Kiba, T., Park, J., Kojima, M., Do, J., … Lee, Y. (2014). Arabidopsis ABCG14 is essential for the root-to-shoot translocation of cytokinin. *Proceedings of the National Academy of Sciences of the United States of America*, *111*(19), 7150–5. http://doi.org/10.1073/pnas.1321519111
Kudo, T., Kiba, T., & Sakakibara, H. (2010). Metabolism and Long-distance Translocation of Cytokinins. *Journal of Integrative Plant Biology*, *52*(1), 53–60. http://doi.org/10.1111/j.1744-7909.2010.00898.x
Lomin, S. N., Yonekura-Sakakibara, K., Romanov, G. A., & Sakakibara, H. (2011). Ligand-binding properties and subcellular localization of maize cytokinin receptors. *Journal of Experimental Botany*, *62*(14), 5149–5159. http://doi.org/10.1093/jxb/err220
Lyons, R., Manners, J. M., & Kazan, K. (2013). Jasmonate biosynthesis and signaling in monocots: A comparative overview. *Plant Cell Reports*, *32*(6), 815–827. http://doi.org/10.1007/s00299-013-1400-y
Makino, S., Kiba, T., Imamura, A., Hanaki, N., Nakamura, A., Suzuki, T., … Mizuno, T. (2000). Genes Encoding Pseudo-Response Regulators: Insight into His-to-Asp Phosphorelay and Orcadian Rhythm in Arabidopsis thaliana. *Plant CellPhysiol*, *41*(6), 791–803. Retrieved from https://watermark.silverchair.com/41-6-791.pdf?token=AQECAHi208BE49Ooan9kkhW_Ercy7Dm3ZL_9Cf3qfKAc485ysgAAAaAwggGcBgkqhkiG9w0BBwagggGNMIIBiQIBADCCAYIGCSqGSIb3DQEHATAeBglghkgBZQMEAS4wEQQMxeV6pjyB-7-oQPoqAgEQgIIBUw5H0fzqH41bAL4YpHagRmJwWtMJ_JIiz1qQvDWsbBjGZt
Martin, R. C., Mok, M. C., Habben, J. E., & Mok, D. W. S. (2001). A maize cytokinin gene encoding an O-glucosyltransferase specific to cis-zeatin. *Proceeding of the National Academy of Sciences, USA*, *98*(10), 5922–5926. Retrieved from https://www.ncbi.nlm.nih.gov/pmc/articles/PMC33314/pdf/pq005922.pdf
Massonneau, A., Houba-Hérin, N., Pethe, C., Madzak, C., Falque, M., Mercy, M., … Laloue, M. (2004). Maize cytokinin oxidase genes: differential expression and cloning of two new cDNAs. *Journal of Experimental Botany*, *55*(408), 2549–2557. http://doi.org/10.1093/jxb/erh274
Miyawaki, K., Tarkowski, P., Matsumoto-Kitano, M., Kato, T., Sato, S., Tarkowska, D., … Kakimoto, T. (2006). Roles of Arabidopsis ATP/ADP isopentenyltransferases and tRNA isopentenyltransferases in cytokinin biosynthesis. *Proceedings of the National Academy of Sciences of the United States of America*, *103*(44), 16598–603. http://doi.org/10.1073/pnas.0603522103
Naseem, M., Kaltdorf, M., & Dandekar, T. (2015). The nexus between growth and defence signalling: auxin and cytokinin modulate plant immune response pathways. *Journal of Experimental Botany*, *66*(16), 4885–4896. http://doi.org/10.1093/jxb/erv297
Nelissen, H., Rymen, B., Coppens, F., Dhondt, S., Fiorani, F., & Beemster, G. T. S. (2013). Chapter 17: Kinematic Analysis of Cell Division in Leaves of Mono- and Dicotyledonous Species: A Basis for Understanding Growth and Developing Refined Molecular Sampling Strategies in Plant Organogensis: Methods and Protocols. *Methods in Molecular Biology*, *959*(2), 247–264. http://doi.org/10.1007/978-1-62703-221-6
R Core Team, T. (2013). R: A language and environment for statistical computing. Vienna, Austria: R Foundation for Statistical Computing. Retrieved from http://www.r-project.org/
Riefler, W. M., Novak, O., Strnad, M., & Schmü Lling, T. (2006). Arabidopsis Cytokinin Receptor Mutants Reveal Functions in Shoot Growth, Leaf Senescence, Seed Size, Germination, Root Development, and Cytokinin Metabolism. *The Plant Cell*, *18*, 40–54. http://doi.org/10.1105/tpc.105.037796
Rodo, A. P., Brugière, N., Vankova, R., Malbeck, J., Olson, J. M., Haines, S. C., … Mok, M. C. (2008). Over-expression of a zeatin O-glucosylation gene in maize leads to growth retardation and

tasselseed formation. *Journal of Experimental Botany*, *59*(10), 2673–2686. http://doi.org/10.1093/jxb/ern137
Sakakibara, H. (2006). Cytokinins: Activity, Biosynthesis, and Translocation. *Annu. Rev. Plant Biol*, *57*, 431–49. http://doi.org/10.1146/
Sakakibara, H., Kasahara, H., Ueda, N., Kokjima, M., Takei, K., Hishiyama, S., … Yamaguchi, S. (2005). Agrobacterium tumefaciens increases cytokinin production in plastids by modifying the biosynthetic pathway in the host plant. *Proceedings of the National Academy of Sciences of the United States of America*, *102*(28), 9972–9977. http://doi.org/10.1073/pnas.95.5.2100
Sakamoto, T., Sakakibara, H., Kojima, M., Yamamoto, Y., Nagasaki, H., Inukai, Y., … Matsuoka, M. (2006). Ectopic Expression of KNOTTED1-Like Homeobox Protein Induces Expression of Cytokinin Biosynthesis Genes in Rice. *Plant Physiology*, *142*(1), 54–62. http://doi.org/10.1104/pp.106.085811
Santner, A., & Estelle, M. (2009). Recent advances and emerging trends in plant hormone signalling. *Nature*, *459*(7250), 1071–1078. http://doi.org/10.1038/nature08122
Schmülling, T., Werner, T., Bartrina, I., Jensen 1$, H., Novák, O., & Strnad, M. (2017). Gain-of-function mutants of the cytokinin receptors AHK2 and AHK3 regulate plant organ size, flowering time and plant longevity. *Plant Physiology Preview. Published On*. http://doi.org/10.1104/pp.16.01903
Sheard, L. B., Tan, X., Mao, H., Withers, J., Ben-Nissan, G., Hinds, T. R., … Zheng, N. (2010). Jasmonate perception by inositol-phosphate-potentiated COI1–JAZ co-receptor. *Nature*, *468*. http://doi.org/10.1038/nature09430
Sun, X., Cahill, J., Van Hautegem, T., Feys, K., Whipple, C., Novák, O., … Nelissen, H. (2017). Altered expression of maize PLASTOCHRON1 enhances biomass and seed yield by extending cell division duration. *Nature Communications*, *8*, 14752. http://doi.org/10.1038/ncomms14752
Sylvester, A. W., Smith, L., & Freeling, M. (1996). Acquisition of Identity in the Developing Leaf, 257–304.
Tam Nguyen, C., Martinoia, E., & Farmer, E. E. (2017). Emerging Jasmonate Transporters. http://doi.org/10.1016/j.molp.2017.03.007
To, J. P. C., Deruère, J., Maxwell, B. B., Morris, V. F., Hutchison, C. E., Ferreira, F. J., … Kieber, J. J. (2007). Cytokinin Regulates Type-A Arabidopsis Response Regulator Activity and Protein Stability via Two-Component Phosphorelay. *The Plant Cell*, *19*, 3901–3914. http://doi.org/10.1105/tpc.107.052662
Ueda, J., & Kato, J. (1982). Inhibition of cytokinin-induced plant growth by jasmonic acid and its methyl ester. *Physiologia Plantarum*, *54*(3), 249–252. http://doi.org/10.1111/j.1399-3054.1982.tb00255.x
Ullmann-Zeunert, L., Stanton, M. A., Wielsch, N., Bartram, S., Hummert, C., Svatoš, A., … Groten, K. (2013). Quantification of growth-defense trade-offs in a common currency: nitrogen required for phenolamide biosynthesis is not derived from ribulose-1,5-bisphosphate carboxylase/oxygenase turnover. *The Plant Journal : For Cell and Molecular Biology*, *75*(3), 417–429. http://doi.org/10.1111/tpj.12210
Veach, Y. K., Martin, R. C., Mok, D. W. S., Malbeck, J., Vankova, R., & Mok, M. C. (2003). O-glucosylation of cis-zeatin in maize. Characterization of genes, enzymes, and endogenous cytokinins. *Plant Physiology*, *131*(3), 1374–80. http://doi.org/10.1104/pp.017210
Vernoud, V., Hajduch, M., Khaled, A. S., Depège, N., & Rogowsky, P. M. (2005). Maize embryogenesis. *Maydica*, *50*(3–4), 469–483. http://doi.org/10.1007/978-1-59745-273-1_2
Walling, L. L. (2000). The Myriad Plant Responses to Herbivores. *Journal of Plant Growth Regulation*, *19*, 195–216. http://doi.org/10.1007/s003440000026
Wang, Y. H., & Irving, H. R. (2011). Developing a model of plant hormone interactions. *Plant Signaling & Behavior*, *6*(4), 494–500. http://doi.org/10.4161/psb.6.4.14558
Werner, T., Motyka, V., Strnad, M., & Schmülling, T. (2001). Regulation of plant growth by cytokinin. *Proceedings of the National Academy of Sciences of the United States of America*, *98*(18), 10487–92. http://doi.org/10.1073/pnas.171304098
Xie, D.-X., Feys, B. F., James, S., Nieto-Rostro, M., & Turner, J. G. (1998). COI1: An Arabidopsis Gene Required for Jasmonate-Regulated Defense and Fertility. *Science*, *280*, 1091–1094. Retrieved from http://science.sciencemag.org/content/sci/280/5366/1091.full.pdf
Yamane, H., Sugawara, J., Suzuki, Y., Shimamura, E., & Takahashi, N. (1980). Syntheses of jasmonic acid related compounds and their structure-activity relationships on the growth of rice seedlings. *Agricultural and Biological Chemistry*, *44*(12), 2857–2864. http://doi.org/10.1080/00021369.1980.10864412
Yan, Y., Christensen, S., Isakeit, T., Engelberth, J., Meeley, R., Hayward, A., … Kolomiets, M. V. (2012).

Disruption of OPR7 and OPR8 Reveals the Versatile Functions of Jasmonic Acid in Maize Development and Defense. *The Plant Cell*, *24*(4), 1420–1436. http://doi.org/10.1105/tpc.111.094151

Yan, Y., Huang, P.-C., Borrego, E., & Kolomiets, M. (2014). New perspectives into jasmonate roles in maize. *Plant Signaling & Behavior*, *9*(10), 1–5. http://doi.org/10.4161/15592316.2014.970442

Yonekura-Sakakibara, K., Kojima, M., Yamaya, T., & Sakakibara, H. (2004). Molecular characterization of cytokinin-responsive histidine kinases in maize. Differential ligand preferences and response to cis-zeatin. *Plant Physiology*, *134*(4), 1654–1661. http://doi.org/10.1104/pp.103.037176.1654

Zahir, Z. A., Asghar, H. N., & Arshad, M. (2000). Cytokinin and its precursors for improving growth and yield of rice. *Soil Biology and Biochemistry*, *33*, 405–408. Retrieved from https://ac-els-cdn-com.eres.library.manoa.hawaii.edu/S0038071700001450/1-s2.0-S0038071700001450-main.pdf?_tid=a6de1929-b449-4235-a7d7-50617f9ab367&acdnat=1525817149_47f49f7f6db2da55f19401fd067bb3b6

Zhang, Y., & Turner, J. G. (2008). Wound-induced endogenous jasmonates stunt plant growth by inhibiting mitosis. *PLoS ONE*, *3*(11). http://doi.org/10.1371/journal.pone.0003699